

# Characterisation of the myeloid cell populations' resident in the porcine palatine tonsil

Jane C. Edwards<sup>1\*</sup>, Ferran Soldevila<sup>2</sup>, Simon P. Graham<sup>3, 4</sup>, Lisa M. Stevens<sup>1</sup>, Bentley Crudgington<sup>1</sup>, Helen R. Crooke<sup>1</sup>, Dirk Werling<sup>5</sup>, Falko Steinbach<sup>1, 4</sup>

<sup>1</sup>Animal and Plant Health Agency (United Kingdom), United Kingdom, <sup>2</sup>Sanford Burnham Prebys Medical Discovery Institute (SBP), United States, <sup>3</sup>Pirbright Institute (BBSRC), United Kingdom, <sup>4</sup>School of Veterinary Medicine, University of Surrey, United Kingdom, <sup>5</sup>Department of Pathobiology and Population Sciences, Royal Veterinary College, United Kingdom

*Submitted to Journal:*  
Frontiers in Immunology

*Specialty Section:*  
Comparative Immunology

*Article type:*  
Original Research Article

*Manuscript ID:*  
384419

*Received on:*  
10 Apr 2018

*Revised on:*  
19 Jul 2018

*Frontiers website link:*  
[www.frontiersin.org](http://www.frontiersin.org)

### *Conflict of interest statement*

The authors declare that the research was conducted in the absence of any commercial or financial relationships that could be construed as a potential conflict of interest

### *Author contribution statement*

FS and BC contributed to the performance of the experiments, FS also contributed to the design of the experiments, performed the data analysis and preparation of the manuscript. JE contributed to the design of the experiments, performed the cell sorts and assisted with the preparation of the manuscript. SG, HC, DW and FSt contributed to the design of the experiments and preparation of the manuscript. All authors reviewed the manuscript.

### *Keywords*

Dendritic Cells, Macrophages, myeloid, porcine, Palatine Tonsil, immunology, pig

### *Abstract*

Word count: 237

Abstract: The palatine tonsil is the portal of entry for food and air, and is continuously subjected to environmental challenges including pathogens which use the tonsil and pharynx as a primary site of replication. In pigs, this includes the viruses causing porcine respiratory and reproductive syndrome, and classical and African swine fever; diseases which have impacted the pig production industry globally. Despite the importance of tonsils in host defence, little is known regarding the phenotype of the myeloid cells resident in the porcine tonsil. Here, we have characterised five myeloid cell populations that align to orthologous populations defined in other mammalian species: a CD4<sup>+</sup> plasmacytoid DC (pDC) defined by expression of the conserved markers E2.2 and IRF-7, a conventional dendritic cell (cDC1) population expressing CADM1<sup>high</sup>CD172a<sup>low</sup> and high levels of XCR1 able to activate allogeneic CD4 and CD8 T cells; a cDC2 population of CADM1<sup>dim</sup> cells expressing FLT3, IRF4 and CSF1R with an ability to activate allogeneic CD4 T cells; CD163<sup>+</sup> macrophages (MΦs) defined by high levels of endocytosis and responsiveness to LPS and finally a CD14<sup>+</sup> population likely derived from a myelo-monocytic lineage, which showed the highest levels of endocytosis, a capacity for activation of CD4<sup>+</sup> memory cells, combined with lower relative expression of FLT3. Increased knowledge regarding the phenotypic and functional properties of myeloid cells resident in porcine tonsil, will enable these cells to be targeted for future vaccination strategies to current and emerging porcine viruses.

### *Funding statement*

The work was supported by Project SE0796 and SE2207 from the UK Department for the Environment, Food and Rural Affairs

### *Ethics statements*

(Authors are required to state the ethical considerations of their study in the manuscript, including for cases where the study was exempt from ethical approval procedures)

Does the study presented in the manuscript involve human or animal subjects: Yes

Please provide the complete ethics statement for your manuscript. Note that the statement will be directly added to the manuscript file for peer-review, and should include the following information:

- Full name of the ethics committee that approved the study
- Consent procedure used for human participants or for animal owners
- Any additional considerations of the study in cases where vulnerable populations were involved, for example minors, persons with disabilities or endangered animal species

As per the Frontiers authors guidelines, you are required to use the following format for statements involving human subjects: This study was carried out in accordance with the recommendations of [name of guidelines], [name of committee]. The protocol was approved by the [name of committee]. All subjects gave written informed consent in accordance with the Declaration of Helsinki.

*For statements involving animal subjects, please use:*

*This study was carried out in accordance with the recommendations of 'name of guidelines, name of committee'. The protocol was approved by the 'name of committee'.*

*If the study was exempt from one or more of the above requirements, please provide a statement with the reason for the exemption(s).*

*Ensure that your statement is phrased in a complete way, with clear and concise sentences.*

Tonsil tissue was supplied by a local abattoir

Blood was granted and approved by the Animal and Plant Health Agency Ethics Committee and all procedures were conducted in accordance with the UK Animals (Scientific Procedures) Act 1986 under Project Licence PPL 70/8343

In review

1 **Title: Characterisation of the myeloid cell populations' resident in the porcine palatine**  
2 **tonsil**

3  
4 **Authors:** Ferran Soldevila<sup>1, #</sup>, Jane C. Edwards<sup>1, \*</sup>, Simon P. Graham<sup>2, 3</sup>, Lisa M. Stevens<sup>1</sup>,  
5 Bentley Crudginton<sup>1</sup>, Helen R. Crooke<sup>1</sup>, Dirk Werling<sup>4</sup>, Falko Steinbach<sup>1, 3</sup>

6 <sup>1</sup>Virology department, Animal and Plant Health Agency, Addlestone, KT15 3NB, United  
7 Kingdom

8 <sup>2</sup>The Pirbright Institute, Ash Road, Pirbright, GU24 0NF, United Kingdom,

9 <sup>3</sup>School of Veterinary Medicine, University of Surrey, Guildford, GU2 7AL, United  
10 Kingdom.

11 <sup>4</sup>Department of Pathobiology and Population Sciences, The Royal Veterinary College,  
12 Hawkshead Lane, North Mymms, Hatfield, Hertfordshire, AL9 7TA.

13  
14 \*Correspondence: Dr: Jane C. Edwards,  
15 Jane.Edwards@apha.gsi.gov.uk

16 #present address: Sanford Burnham Prebys Medical Discovery Research Institute, 10901  
17 North Torrey Pines Rd La Jolla, CA 92037 United States.

18 **Keywords: Dendritic cells, macrophages, myeloid, porcine, palatine tonsil,**  
19 **immunology, pig,**

20  
21 **Abstract:** The palatine tonsil is the portal of entry for food and air, and is continuously  
22 subjected to environmental challenges including pathogens which use the tonsil and pharynx  
23 as a primary site of replication. In pigs, this includes the viruses causing porcine respiratory  
24 and reproductive syndrome, and classical and African swine fever; diseases which have  
25 impacted the pig production industry globally. Despite the importance of tonsils in host  
26 defence, little is known regarding the phenotype of the myeloid cells resident in the porcine  
27 tonsil. Here, we have characterised five myeloid cell populations that align to orthologous  
28 populations defined in other mammalian species: a CD4<sup>+</sup> plasmacytoid DC (pDC) defined by  
29 expression of the conserved markers E2.2 and IRF-7, a conventional dendritic cell (cDC1)  
30 population expressing CADM1<sup>high</sup>CD172a<sup>low</sup> and high levels of XCR1 able to activate  
31 allogeneic CD4 and CD8 T cells; a cDC2 population of CADM1<sup>dim</sup> cells expressing FLT3,  
32 IRF4 and CSF1R with an ability to activate allogeneic CD4 T cells; CD163<sup>+</sup> macrophages  
33 (MØs) defined by high levels of endocytosis and responsiveness to LPS and finally a CD14<sup>+</sup>  
34 population likely derived from a myelo-monocytic lineage, which showed the highest levels  
35 of endocytosis, a capacity for activation of CD4<sup>+</sup> memory cells, combined with lower  
36 relative expression of FLT3. Increased knowledge regarding the phenotypic and functional  
37 properties of myeloid cells resident in porcine tonsil, will enable these cells to be targeted for  
38 future vaccination strategies to current and emerging porcine viruses.



## 41 Introduction

42 Pigs are both an important source of meat globally and represent a valuable biomedical  
43 model. The porcine and human immune systems present evolutionary convergent features  
44 and, as such, pigs represent an important model for disease pathogenesis and vaccine  
45 development (Meurens et al., 2012). In pigs, however, the mononuclear phagocyte system  
46 (MPS) of dendritic cells (DCs) and macrophages (M $\phi$ s) is less characterised than those of  
47 either mice or humans. As a first line of defence to pathogen invasion, a clearer  
48 understanding of these cells, and how they might be identified, will facilitate our  
49 understanding of host-pathogen interaction in this species.

50 DCs are the sentinels of the immune system, they possess a distinct morphology and a unique  
51 capacity to activate naïve T cell populations (Steinman and Cohn, 1973, Steinman et al.,  
52 1978). They are also able to coordinate or regulate the adaptive immune system, depending  
53 on the antigenic signals and microbial environment at the time of antigen uptake. DCs are  
54 classified into two populations; plasmacytoid DCs (pDCs), specialising in the production of  
55 type I IFNs and conventional DC (cDCs), which are potent antigen-presenting cells (APCs)  
56 (Salio et al., 1999, Cella et al., 1999). Two sub populations of cDCs (cDC1s and cDC2s)  
57 have been described in mouse and human (Schlitzer and Ginhoux, 2013) and more recently in  
58 other mammalian species (Marquet et al., 2011, Marquet et al., 2014, Manh et al., 2013,  
59 Crozat et al., 2010a, Vu Manh et al., 2015a). Across species, these populations share  
60 expression of several conserved phenotypic markers, cytokine secretion profiles and specific  
61 functionalities. However, while cDC1s are presumed unique in their capacity to cross-  
62 present antigen to CD8 T cells in mice (den Haan et al., 2000), both cDC1 and cDC2 appear  
63 able to cross present in humans, depending on specific TLR stimulation and the local  
64 cytokine environment (Nizzoli et al., 2013, Jongbloed et al., 2010) indicating that these  
65 subsets may have some redundant functions. During an immune response an additional  
66 ‘inflammatory’ DC subset has been identified (moDC) in lymphoid tissue which in mice are  
67 recruited from circulating Ly6Chi monocytes (Leon et al., 2007). This population is capable  
68 of presenting antigen to both CD4 and CD8 T cells and inducing T<sub>H</sub>1, T<sub>H</sub>2 (Leon et al., 2007,  
69 Hammad et al., 2010) or T<sub>H</sub>17 mediated responses (Segura and Amigorena, 2013, Segura et  
70 al., 2013).

71 M $\phi$ s are also resident in lymphoid (and non-lymphoid) tissues that have developed from  
72 either early erythro-myeloid progenitors from the extra-embryonic yolk sac or which have  
73 matured from circulating monocytes (Ginhoux and Guilliams, 2016). These cells are  
74 characterised by their variable expression of CD14, their responses to TLR4 stimulation,  
75 active phagocytic properties and their production of inflammatory cytokines such as TNF- $\alpha$ ,  
76 IL1 $\beta$ , IL-6, IL-8 and IL-12 (Fairbairn et al., 2011).

77 In pigs, DCs and M $\phi$ /monocyte populations have been characterised successfully in skin  
78 (Marquet et al., 2011, Marquet et al., 2014), blood (Auray et al., 2016, Edwards et al., 2017,  
79 Vu Manh et al., 2015b), lungs (Maisonnette et al., 2016) and lymphoid tissue (Parra-Sanchez  
80 et al., 2018). In the skin, CD172a<sup>neg</sup>CD163<sup>neg</sup> cells were identified as cDC1 cells given their  
81 high expression of CADM1 and XCR1. The CD163<sup>low</sup> CD172a<sup>pos</sup> cells expressed markers  
82 ZBTB46 and FLT3 aligning them with mouse and human cDC2s. A population of CD163<sup>pos</sup>  
83 porcine dermal dendritic cell were also classified as similar to human CD14<sup>+</sup> dermal DCs  
84 (Marquet et al., 2011, Marquet et al., 2014). Applying a similar panel of antibodies, cDC1  
85 and cDC2 populations were identified in porcine lungs (Maisonnette et al., 2016).

86 The palatine tonsil is positioned at the opening of the respiratory and gastrointestinal tract,  
87 providing an immunological barrier (consisting of macrophages, dendritic cells and  
88 lymphocytes) equipped to induce an immune response. In human tonsils, three populations  
89 of DCs have been described; pDCs, cDC1s and cDC2s (Segura et al., 2012) and more lately  
90 cDC1s and cDC2s have been identified in the porcine tonsil (Parra-Sanchez et al., 2018).  
91 However, the different populations that make up the milieu of myeloid cells which reside in  
92 the porcine tonsil has received little attention. It is these cells which form the first line of  
93 defence to air-borne pathogens and viruses and are tasked with ensuring an appropriate  
94 immune response is relayed following encounter with pathogen or commensal derived  
95 microbes. Here, we successfully employed multi-parameter flow cytometry to  
96 immunophenotype five distinct myeloid cell populations resident in porcine tonsil. To  
97 further characterise these populations, we localised these subsets *in situ* using confocal  
98 microscopy, sorted and assessed these cells functionally and, by way of RT-qPCR, evaluated  
99 the expression of conserved markers expressed by various myeloid cells populations.  
100 Through these analyses we identified three orthologous classical DC subsets (pDCs, cDC1s  
101 and cDC2s), MØs, and a CD14 positive subset with characteristics interrelating with DCs and  
102 MØs, consistent with a monocyte derived DC population.

103

## 104 **Materials and Methods**

### 105 **Animals and tissue collection**

106 Pig palatine tonsils were obtained from a local abattoir and transported at room temperature  
107 to the laboratory. Pigs were typically 6-12 month-old Large White or Large White cross  
108 breeds. For the mixed leukocyte reaction (MLR), peripheral blood mononuclear cells  
109 (PBMC) were isolated from blood obtained from animals kept at the Animal and Plant Health  
110 Agency (APHA) facilities under housing and sampling regulations approved by the APHA  
111 Animal Welfare and Ethical Review Board and conducted in accordance with the Animals  
112 (Scientific Procedures) Act, UK.

113

### 114 **Tonsil cell isolation and lymphocyte depletion**

115 Porcine palatine tonsils were dissected from the surrounding tissue and washed twice with  
116 PBS before being placed in a Petri dish. Tonsils were then cut into small fragments while  
117 submerged in PBS and further dissociated using the perforated end of a syringe plunger. The  
118 resulting cell suspension was filtered through a 40 µm cell strainer (Corning, Sigma-Aldrich,  
119 Gillingham, UK). Mononuclear cells were then separated over a Ficoll gradient (1.077 g/l,  
120 Sigma Aldrich). Myeloid cells were enriched by magnetic depletion of lymphocytes using  
121 anti-CD3 (clone 8E6), anti-CD8α (clone PT36A) (both from Washington State University  
122 Monoclonal Antibody Center, Pullman, USA), anti-CD21 (clone BB6-11C9.6, Cambridge  
123 Bioscience, Cambridge, UK), and anti-IgM (Clone K52 1C3; Bio-Rad AbD Serotec Ltd,  
124 Oxford, UK) mAbs followed by incubation with anti-mouse IgG1 magnetic beads and  
125 separation through LD columns (Miltenyi Biotec, Bisley, UK) according to the  
126 manufacturer's instructions.

127

## 128 **Flow cytometry and cell sorting**

129 For phenotypic analysis of tonsillar myeloid cells, cell surface staining was performed in  
130 three consecutive steps. Cells were initially incubated with the same lymphocyte lineage  
131 antibodies as described above (anti-CD3, anti-CD8 $\alpha$ , anti-CD21 and anti-IgM, all of an IgG1  
132 isotype) and anti-CD4-PerCP-Cy5.5 (clone 72-12-4; BD Pharmingen, Oxford, UK), CD14  
133 PE Texas Red (clone Tük4; Fisher Scientific, Loughborough, UK), MHC class II-DR (clone  
134 2E9/13; Bio-Rad AbD Serotec Ltd.) labelled with Zenon anti-mouse IgG2b PE (Life  
135 Technologies, Paisley, UK) and anti-Syn-CAM (TSLC1/CADM1) biotinylated antibody  
136 (Clone 3E1; MBL, Caltag Medsystems, Buckingham UK). Following incubation for 10 mins  
137 at room temperature (rt), cells were washed then labelled with a secondary anti-mouse IgG1  
138 Brilliant Violet 421 (Clone RMG1-1; Bio Legend London, UK) and streptavidin Brilliant  
139 Violet 605 (BioLegend) again for 10 mins at rt. Finally, cells were stained with anti-CD172a  
140 FITC (clone BL1H7; Bio-Rad AbD Serotec Ltd) and anti-CD163 conjugated to anti-mouse  
141 IgG1 Zenon APC (Life Technologies), again for 10 mins at rt. Data was acquired on a LSRII  
142 Fortessa (BD Biosciences Oxford, UK) and collected in FACS Diva Software (BD  
143 biosciences). All analysis and compensation was performed using Kaluza Software  
144 (Beckman Coulter, High Wycombe UK).

145 For several downstream analyses the identified myeloid populations were stained as  
146 described above and sorted using a MoFlo Astrios (Beckman Coulter). Sorted populations  
147 were collected in RPMI-1640 medium supplemented with 40% foetal bovine serum and  
148 100U/mL of penicillin, 100 $\mu$ /mL streptomycin (Life Technologies). For mRNA extraction,  
149 cells were pelleted and supernatant removed before snap freezing in liquid nitrogen. Cells  
150 were stored at -80°C until RNA extraction. Typically, between 3-8x10<sup>5</sup> cells were analysed  
151 by flow cytometry (per sample) depending on the experiment. For sorting, between 5-10x10<sup>6</sup>  
152 cells were sorted depending on the pig.

153

## 154 **TLR stimulation and intracellular cytokine staining**

155 Lymphocyte-depleted tonsillar mononuclear cells from 8 pigs (obtained from an abattoir) and  
156 isolated as described above and seeded in round-bottom 96-well plates in 200 $\mu$ l of complete  
157 RPMI-1640 (cRPMI), supplemented with 10% FBS, 100U/ml penicillin and 100 $\mu$ g/ml  
158 streptomycin (Life Technologies). Cells were cultured for 10 hours with either CpG  
159 ODN21798 (to stimulate TLR9) (Miltényi Biotec, Bisley UK) at 10 $\mu$ g/ml, Poly I:C HMW  
160 (To stimulate TLR3) (Invivogen, Toulouse, France) at 10 $\mu$ g/ml, LPS (to stimulate TLR 4)  
161 (Invivogen,) at 1 $\mu$ g/ml or media supplemented with recombinant IL-3 at 10ng/ml at 37°C +  
162 5% CO<sub>2</sub> . Following 4 hours of culture GolgiPlug® (BD Biosciences) was added and cells  
163 incubated for a further 6 hours. Cells were then stained as described above with the exception  
164 of applying non-biotinylated anti-Syn-CAM (TSLC1/CADM1) (Clone 3E1; MBL) (Caltag  
165 Medsystem) labelled with anti-chicken IgY APC (Jackson ImmunoResearch, Newmarket,  
166 UK) and CD163 conjugated with Zenon anti-mouse IgG1 APC AlexaFluor750 (Life  
167 Technologies, Paisley, UK). For intracellular staining, cells were treated with BD  
168 Cytotfix/Cytoperm™ (BD Biosciences, Oxford, UK) for 20 minutes at 4°C washed with BD  
169 Perm/Wash™ before staining with either biotinylated anti-IL-12 (R&D Systems, Abingdon,  
170 UK) or directly conjugated anti-TNF- $\alpha$  Brilliant Violet 605 (eBioscience, Hatfield, UK) in  
171 Perm/Wash™ buffer. IL-12 staining was detected by addition of streptavidin BV605 for 30  
172 minutes at 4°C. Finally, cells were washed with Perm/Wash™ and resuspended in PBS  
173 supplemented with 2% FBS. Staining was assessed on the LSRII Fortessa.

174

### 175 **OVA processing by tonsillar myeloid cells**

176 Lymphocyte-depleted tonsillar mononuclear cells from 4 pigs were seeded at  $2.5 \times 10^5$   
177 cells/well in cRPMI-1640. DQ-OVA FITC (Life technologies) at a final concentration of  
178  $2 \mu\text{g/ml}$ , or media (as a negative control), were added in triplicate to the cells and cultured at  
179 either  $37^\circ\text{C}$  or  $4^\circ\text{C}$  (to confirm active uptake of antigen). After 1.5 hours incubation, cells  
180 were stained using the phenotypic staining protocol described above with the exception that  
181 CD172a-FITC was substituted with CD172a (non-conjugated) labelled with anti-mouse IgG1  
182 APC Zenon labelling kit (Life Technologies). Samples were acquired on the LSRII Fortessa.

183

### 184 **Mixed lymphocyte reaction**

185 For allogeneic T cell stimulation experiments, PBMC were stained using CellTrace™ Violet  
186 Cell Proliferation Kit (Life Technologies)  $10^6$  cells were incubated with  $5 \mu\text{M}$  of dye in PBS  
187 (at  $37^\circ\text{C}$  for 20 minutes). Cells were washed and resuspended in cRPMI-1640 and incubated  
188 for a further 10 minutes. Sorted myeloid cells were seeded at  $5 \times 10^3$  cells/well, and added to  
189 ?stained PBMC at  $5 \times 10^4$  in a final volume of  $200 \mu\text{l}$  in either duplicate or triplicate depending  
190 on the number of myeloid cells successfully sorted. Negative and positive controls were  
191 included using CellTrace™ Violet stained PBMCs with media and pokeweed mitogen  
192 (PWM; Sigma-Aldrich) at a concentration of  $10 \mu\text{g/ml}$  respectively. After 5-day culture, cells  
193 were washed and stained with anti-CD4-PerCP-Cy5.5 anti-CD8a-PE (clone76-2-11; BD  
194 Pharmingen) and analysed by flow cytometry. Reduction of CellTrace™ Violet staining was  
195 evaluated as an indicator of cell proliferation, whereby  $\text{CD4}^+\text{CD8a}^-$  (Naïve  $\text{CD4}^+$  T helper  
196 cells),  $\text{CD4}^-\text{CD8a}^+$  (cytotoxic T lymphocytes) and  $\text{CD4}^+\text{CD8a}^+$  ( $\text{CD4}^+$  T memory cells) were  
197 identified and the percentage of proliferating cells in each population determined. To identify  
198 the relative proliferation index of each of the T cell populations, a value of 100 was assigned  
199 to the myeloid cell population stimulating the maximum percentage of proliferating cells and  
200 other populations where normalised to this.

201

### 202 **RNA extraction and quantitative RT-PCR (RT-qPCR)**

203 Total RNA from FACSorted cell populations was extracted using the RNeasy Micro Kit  
204 (Qiagen, Manchester, UK) according to the manufacturer's instructions. Genomic DNA was  
205 removed using the RNase-Free DNase Set (Qiagen, Manchester, UK) during RNA  
206 extraction. RNA was reverse transcribed using random hexamers and the M-MLV reverse  
207 transcriptase (Promega, Southampton, UK). All qPCR reactions were performed using  
208 SYBR® Select Master Mix (ThermoFisher Scientific, Paisley, UK) in a final volume of  $20 \mu\text{l}$ .  
209 The primers used are listed in Table 1. Analysis was performed using the MxPro QPCR  
210 Software (Agilent Technologies, Stockport, UK) and the cycle threshold ( $C_T$ ) values for each  
211 amplification curve were determined. Relative quantification was calculated using the  $\Delta C_T$   
212 method and normalized to the expression of  $\beta$ -actin mRNA. In order to compare data sets the  
213 arbitrary units (AU), for each animal the cell population with the highest level of expression  
214 of each gene was considered 100 and the remaining populations were normalised to it as  
215 shown by Maisonnasse and colleagues (Maisonnasse et al., 2016).

216

## 217 **Confocal microscopy**

218 Optimum Cutting Temperature (OCT, Tissue-Tek) treated tissue blocks were submerged in  
219 isopentane at -80°C until frozen and cut into 6-10µm thick sections by cryo-sectioning (Leica  
220 RM2135 cryotome). Sections were then transferred on to microscopy slides and fixed in  
221 absolute ethanol before storing at -80°C prior to processing.

222 The mounted tissue sections were placed into Sequenza clips (Shandon, Paisley, UK) and  
223 then incubated in 5% (w/v) normal goat serum (Sigma-Aldrich) in TBS-T either overnight  
224 (panel 1) or for 30 minutes (panel 2) at room temperature in the sequenza staining rack. For  
225 identification of CD14<sup>+</sup> cells and pDCs, panel 1 antibodies were applied, these included  
226 lineage antibodies (as described above; conjugated to biotin), Anti-CD4α AF488 (Clone  
227 MIL17; Bio-Rad) and Anti-CD14 dylight 550 (Clone Tük4;), all antibodies were conjugated  
228 to their respective protein/flouochrome using Lightning link labelling kits (Expedeon). Panel  
229 1 antibodies were applied to the slides for 120 minutes at 37°C then washed 3 times in TBST  
230 before incubation with streptavidin-APC (Bio-Rad) at 37°C for a further 90 minutes before  
231 washing again for 3 times in TBST. The slides were then incubated with 4',6-Diamidino-2-  
232 Phenylindole, Dihydrochloride (DAPI, Thermo Fisher) diluted 1/10000 in deionised water at  
233 room temperature for 30 minutes before washing twice. For detection of cDC1s, cDC2s and  
234 macrophages, panel 2 antibodies were applied for 30 minutes at room temperature which  
235 included the lineage antibodies (unconjugated). After washing 3 times with TBST, anti-  
236 mouse IgG1-BV421 (Clone RMG1-1; Bio Legend) was applied for detection. After further  
237 washing steps, anti-CD172a FITC (clone BL1H7) anti-Syn-CAM (TSLC1/CADM1)  
238 biotinylated antibody (Clone 3E1) and anti-CD163 (clone 2A10/11; Bio-Rad) conjugated to  
239 anti-mouse IgG1 Zenon APC (Life Technologies) were added for 30 mins at room  
240 temperature. Slides were then washed before applying streptavidin Brilliant Violet 605  
241 (BioLegend) for 30 minutes at room temperature.

242 Finally, all the slides were washed twice with deionised water before being removed from the  
243 Sequenza clips and coverslips mounted with Pro-Long Gold anti-fade mounting media  
244 (Thermo Fisher). The slides were allowed to dry in the dark overnight and then sealed with  
245 nail varnish. Slides were imaged using the Leica SP2 confocal microscope.

246

## 247 **Statistical analysis**

248 GraphPad Prism 6.0 (GraphPad software, La Jolla, California, USA) was used for the  
249 analysis of data sets. Statistical tests applied to each data set are indicated in the relevant  
250 figure legend.

251

252

253

## 254 **Results**

### 255 **Identification of five distinct populations of myeloid cells in porcine tonsil**

256 A panel of markers that had previously defined DCs and M $\Theta$  populations in various species  
257 (Croizat et al., 2010b, Contreras et al., 2010, Marquet et al., 2011) was selected to determine  
258 the presence of myeloid populations resident in porcine tonsil (Figure 1). Since myeloid cells  
259 are comparatively rare in secondary lymphoid tissues they were enriched by antibody-  
260 associated magnetic depletion of cells expressing the lymphocyte lineage markers CD3 (T  
261 cells), CD8 $\alpha$  (NK cells), CD21 and sIgM (B cells). Following doublet discrimination (Figure  
262 1A), live cells were identified and remaining lineage positive cells excluded. After selection  
263 of MHC class II positive cells, a candidate pDC population was identified as CD172a<sup>low</sup>CD4<sup>+</sup>  
264 MHC II<sup>low</sup>, which corresponds to the defined porcine plasmacytoid dendritic cells (pDCs)  
265 (Summerfield et al., 2003) (Figure 1B). The remaining cells delineated into CD172a<sup>neg/low</sup>,  
266 CADM1<sup>high</sup>, MHC II<sup>hi</sup> cells representing a putative cDC1 population. The CD172a<sup>high</sup> cells  
267 could be divided into three distinct populations whereby CD172a<sup>hi</sup>, CD14<sup>-</sup>, CD163<sup>-</sup>MHC II<sup>hi</sup>,  
268 CADM1<sup>low</sup> phenotypically resembled a cDC2-like population (cDC2); CD172a<sup>hi</sup>, CD163<sup>-</sup>,  
269 CD14<sup>+</sup>, MHC II<sup>hi</sup> cells were believed to be a monocyte derived population (CD14<sup>+</sup> cells),  
270 while CD172a<sup>hi</sup>, CD163<sup>+</sup>, CD14<sup>-</sup>, MHC II<sup>hi</sup> cells represented a macrophage-like population  
271 (M $\Theta$ s).

272 To assess the relative frequency of each of the five cell populations in the tonsil, the  
273 percentage of each subset was determined within the MHC-II positive fraction (Figure 1C).  
274 The CD14<sup>+</sup> cells were the most frequent DC population at 6.75 $\pm$ 2.20%, followed by cDC1s  
275 (2.54 $\pm$ 1.49%), M $\Theta$ s (1.52 $\pm$ 0.71%), cDC2s at 1.00 $\pm$ 0.74% and pDCs being the rarest  
276 population (0.32 $\pm$ 0.34%).

277

### 278 **Expression of conserved myeloid cell markers assessed by qPCR**

279 The key aim of this study was to align the identified myeloid cell populations with their  
280 human and mice counterparts and to correlate them with similar populations in porcine skin  
281 (Marquet et al., 2011, Marquet et al., 2014), lungs (Maisonasse et al., 2016) blood (Auray et  
282 al., 2016) (Edwards et al., 2017) and lymphoid tissue, **including tonsil** (Parra-Sanchez et al.,  
283 2018). However, not all proteins can be assessed by flow cytometry in pigs, due to lack of  
284 suitable antibodies. Several genes were therefore selected for further evaluation by gene  
285 expression. Expression of these markers is conserved across DC subsets and/or M $\Theta$   
286 populations in different species (Maisonasse et al., 2016) and their appearance on porcine  
287 tonsil myeloid cells was assessed by RT-qPCR. The putative pDC population were found to  
288 express high levels of E2.2, a gene important in pDC development (Auray et al., 2016), and  
289 also IRF7 and FLT3 (Figure 2). The cDC1-like cells expressed the cDC marker ZBTB46  
290 (Satpathy et al., 2012) and the highest levels of the bona fide DC marker FLT3. These cells  
291 also demonstrated expression of XCR1, a gene considered to be a hallmark of cDC1 (Bachem  
292 et al., 2010). The cDC2-like cells expressed FLT3 and ZBTB46, and high levels of IRF4 and  
293 SIRP $\alpha$ , genes involved in cDC2 development. Monocyte/M $\Theta$  related genes including IL-1B,  
294 MAFB and CSF1R were also expressed by the cDC2-like population, albeit at lower levels  
295 than observed in M $\Theta$ s. Notably, the CD14<sup>+</sup> cells expressed DC related genes FLT3 and  
296 ZBTB46, but also macrophage related genes IL-1B, MAFB and CSF1R. IRF4 expression  
297 was also observed although at lower levels than associated with the cDC2-like cells. Finally,  
298 as expected, macrophages failed to express FLT3 but did express ZBTB46 but at slightly  
299 lower levels than the cDC and CD14<sup>+</sup> cells. Unsurprisingly, the putative macrophage

300 population expressed the highest levels of IL-1B, MAFB and CSF1R and also the highest  
301 levels of SIRP $\alpha$ .

302

### 303 **MHC-II and costimulatory molecule expression on isolated and cultured tonsillar** 304 **myeloid cells**

305 DCs are characterised by an ability to activate naïve T cells due to their constitutive  
306 expression of MHC class II and costimulatory proteins (Banchereau and Steinman, 1998). At  
307 steady state, and immediately after isolation, the highest levels of MHC class II were  
308 associated with cDC1s, closely followed by cDC2. The lowest levels of MHC class II were  
309 associated with pDCs (Figure 3). The highest levels of CD80/86 expression were associated  
310 with the M $\Theta$ -like populations while again the lowest levels were expressed by pDC. To  
311 evaluate whether these markers might increase in expression as the cells develop a more  
312 mature phenotype, cells were cultured for 4 hours in the absence of specific stimulation. For  
313 both pDCs and M $\Theta$ s, there was only a modest increase in CD80/86 and MHC-II expression  
314 levels as demonstrated by the MFI (mean fluorescence intensity), which was not statistically  
315 significant. In contrast, CD14<sup>+</sup> cells, cDC1-like and cDC2-like cells all demonstrated a  
316 significant upregulation of both these markers. CD14<sup>+</sup> cells increased expression levels of  
317 CD80/86 from 2.111 $\pm$ 0.172 to 5.232 $\pm$ 0.941, and MHC-II expression from 47.141 $\pm$ 13.775 to  
318 234.164 $\pm$ 53.693. cDC1-like cells increased their CD80/86 expression from 1.742 $\pm$ 0.328 to  
319 4.715 $\pm$ 1.821 and MHC-II from 97.517 $\pm$ 15.997 to 387.157 $\pm$ 82.053 and finally cDC2-like  
320 cells increased CD80/86 from 3.065 $\pm$ 0.460 to 7.013 $\pm$ 2.514 and MHC-II from 72.528 $\pm$ 13.334  
321 to 337.820 $\pm$ 71.097 (Figure 3).

322

### 323 **Evaluation of TLR expression across the five populations of myeloid cells**

324 Myeloid cells express a broad repertoire of pathogen recognition receptors including toll-like  
325 receptors (TLRs). Binding of the TLRs serves as a danger signal resulting in myeloid cell  
326 activation and ultimately a trigger for activation of the adaptive immune system. Others have  
327 demonstrated that DCs and M $\Theta$  cell populations express conserved TLR profiles; for  
328 example, human and mouse M $\Theta$ s are associated with high levels of TLR4 expression (Vaure  
329 and Liu, 2014) while cDC1 cells express TLR3 (Reynolds and Haniffa, 2015). To further  
330 evaluate the phenotypes of the five myeloid cell populations the TLR profile (TLR1-10) of  
331 each of the populations was determined by RT-PCR (Figure 4). TLR5 expression was below  
332 the limit of detection and therefore the data is not shown. TLR1, 8 and 10 were expressed at  
333 comparatively similar levels across all cell populations with the exception of pDCs, which  
334 expressed much lower levels. TLR2, 4 and 6 were expressed at significantly higher levels on  
335 the M $\Theta$ -like cells compared to all other populations. TLR2, 4 and 6 were also expressed,  
336 albeit at a lower level, on the putative CD14<sup>+</sup> cells and the cDC2-like cells, while negligible  
337 levels of expression were seen on cDC1-like and pDCs. Similarly, to human and mouse  
338 pDCs, TLR7 and 9 were expressed at high levels on porcine tonsil pDC populations.  
339 However, TLR7 was not restricted to pDCs, but was also expressed by M $\Theta$ -like cells, cDC2  
340 and CD14<sup>+</sup> cells (again at a lower level). This is consistent with a previous report  
341 demonstrating expression of TLR7 by porcine blood monocytes and cDC2s, in addition to  
342 pDCs (Auray et al., 2016). Another difference to human and mouse cells was the very high  
343 level of expression of TLR3 on pDCs, which is otherwise restricted to cDC1 cells, yet in pigs  
344 was expressed at very low levels on tonsillar cDC1s. Notably cDC1s expressed TLR9 at  
345 comparable levels to pDCs.

346

## 347 **Evaluation of antigen processing, T cell stimulatory capacity and cytokine responses to** 348 **TLR stimulation**

349 One of the cardinal functions of myeloid cells is their ability to process and present antigen in  
350 order to activate T cells. To evaluate the antigen processing capacity of each of the five  
351 identified populations we assessed the uptake and processing of quenched DQ-OVA-FITC  
352 particles by the myeloid cell populations following 1.5 hours of culture (Figure 5A). Both  
353 pDCs and cDC1s were the least efficient at processing DQ-OVA-FITC particles followed by  
354 the cDC2 population. In contrast the CD14<sup>+</sup> cells were the most efficient followed by the  
355 MØs. Next, to assess the relative ability of the myeloid cells to activate T cells we compared  
356 the capacity of the different sub-populations to activate allogeneic CD4<sup>+</sup> and CD8<sup>+</sup> T cells in  
357 a mixed leucocyte reaction (MLR). The cDC1-like and cDC2-like populations were most  
358 able to stimulate naïve CD4<sup>+</sup> T cells with the DC2 cells showing the highest stimulatory  
359 capacity (Figure 5B). The cDC1 and cDC2 like populations were most effective at  
360 stimulating CD8<sup>+</sup> T cell proliferation however, while cDC1-like cells showed a tendency  
361 toward the higher proliferation index, this was not found to be statistically significant.  
362 Finally, the cDC1s, cDC2s and the CD14<sup>+</sup> cells were equally able to stimulate memory CD4<sup>+</sup>  
363 T cells (shown by others to express a CD4/CD8 double positive phenotype) (Zuckermann and  
364 Husmann, 1996) while the pDCs and MØs showed a relatively low capacity for stimulating  
365 allogeneic T cells. Also, since the PBMC were stained with antibodies to CD4 and CD8  
366 (and didn't include CD3), we cannot discount the possibility that NK cells will also be  
367 included within the CD8 T cell population.

368 Finally, we evaluated how the myeloid cells might respond to TLR stimulation. Cells  
369 enriched in myeloid subsets (through depletion of cells expressing lineage markers ) were  
370 cultured with CpG (ODN21798) which is a TLR9 agonist, Poly I:C as a TLR3 agonist and  
371 LPS as a TLR4 agonist and assessed for expression of IL-12 and TNF- $\alpha$  by flow cytometry.  
372 Due to decreased cell viability following 10 hours culture, pDCs had to be excluded from  
373 these analyses. The results showed that cDC1s secreted IL-12 following CpG stimulation  
374 (Figure 5C,D), most likely reflecting TLR9 expression on this cell population (Figure 4).  
375 However, CD14<sup>+</sup> cells also responded to CpG stimulation secreting both IL-12 and TNF- $\alpha$   
376 despite their comparatively low levels of TLR9 expression. Similarly cDC1-like cells  
377 secreted the highest levels of IL-12 following Poly I:C stimulation despite an apparent low  
378 abundance of TLR3 associated with these cells.

379

## 380 ***In situ* localisation of myeloid cell populations in tonsils**

381

382 To further evaluate the 5 myeloid cell populations identified in the tonsil, we investigated  
383 their sub-localisation *in situ*. To minimise spectral overlap between the fluorophores, the 5  
384 myeloid cell populations were identified across two separate panels; panel 1 to identify CD14<sup>+</sup>  
385 cells and pDCs and panel 2 to identify cDC1s, cDC2s and macrophages (Figure 6 and 7).

386

387 The tonsil regions assessed included the tonsillar crypts (C), lymphoid follicles (F), the  
388 interfollicular area (IFA) and the epithelia (E). Using panel 1, pDC's were detected in the  
389 IFA and less frequently in the follicles (data not shown) and beneath the squamous epithelia  
390 lining the crypt (Figure 6). Similarly, CD14<sup>+</sup> cells were located mostly in the IFA and



391 beneath the epithelia of the crypt. On occasion these cells were detected in the follicle.  
392 Neither of these populations could be detected in the epithelium or connective tissue.  
393 Applying panel 2 (Figure 7), cDC1s were observed in the area surrounding the crypt, the  
394 follicles, the connective tissue and also the IFA. cDC2s were restricted to the crypt  
395 epithelium and the follicles. Finally, macrophages were found in the crypt lumen leading to  
396 the outside of the tissue and also in the area surrounding the crypt. They were particularly  
397 abundant on the edge of the tonsils, where they could be detected in the epithelium, the sub-  
398 epithelial connective tissue, sinusoid and the adjacent lymphoid tissue. Clearly macrophages  
399 and CD14<sup>+</sup> cells were positioned close to areas where pathogens might be expected to enter the  
400 tonsil.

401

## 402 Discussion

403 Understanding the complexity of myeloid cell populations in pigs has become an important  
404 topic both in furthering our understanding on how these cells coordinate the adaptive immune  
405 system but also with respect to the opportunities that these cells offer as targets to modulate  
406 the immune response e.g. in vaccine development. Specialised subsets of DCs and  
407 monocyte/MØs have now been comprehensively studied in various species and tissues and  
408 the evolutionary conserved patterns of cell phenotype and function established between  
409 human and rodents have generally remained true across livestock and companion animal  
410 species (Robbins et al., 2008, Crozat et al., 2010b, Contreras et al., 2010, Marquet et al.,  
411 2011).

412

413 Porcine myeloid cell populations have recently been characterised in blood (Edwards et al.,  
414 2017, Auray et al., 2016), lung (Maisonasse et al., 2016) and skin (Marquet et al., 2011,  
415 Marquet et al., 2014) however, little is known regarding their frequency and phenotype in  
416 secondary lymphoid organs, including the tonsil. A very recent study reported the presence  
417 of two resident dendritic cell populations; cDC1s and cDC2s in swine palatine tonsil (Parra-  
418 Sanchez et al., 2018), however, to our knowledge, this is the first study to apply multi-colour  
419 flow cytometry, confocal microscopy in addition to molecular and functional assays to  
420 delineate 5 distinct populations of myeloid cells resident in porcine tonsil.

421

422 The work presented here demonstrates clear homologies of porcine tonsillar myeloid cells  
423 with myeloid populations described in other porcine tissue and human tonsil. The myeloid  
424 cells were immature in the steady state, a feature consistent with the orthologous population  
425 in human tonsil (Segura et al., 2012). Porcine pDCs were identified as MHC-II<sup>low</sup>  
426 CD172a<sup>low/neg</sup> CD4<sup>+</sup> CADM1<sup>-</sup> CD14<sup>-</sup> CD163<sup>-</sup> as previously described in porcine blood  
427 (Auray et al., 2016, Edwards et al., 2017). True to their assigned lineage, PCR analysis  
428 confirmed expression of FLT3, a tyrosine kinase receptor (necessary for development of DCs  
429 from progenitor cells (Karsunky et al., 2003)) and E2-2, a specific transcription regulator of  
430 pDCs development in mouse human and pig (Cisse et al., 2008, Auray et al., 2016). pDCs  
431 also expressed IRF7 and TLRs 7 and 9 as observed in human pDCs (Kastenmuller et al.,  
432 2014) and demonstrated a low antigen processing and T cells stimulatory capacity as shown  
433 in other porcine tissue (Summerfield et al., 2003) (Jamin et al., 2006, Edwards et al., 2017).  
434 The cDC1-like cell population was identified by the high expression of MHC-II, the low/neg  
435 expression of CD172a, negative expression of CD4, CD14 and CD163 and high expression  
436 of CADM1 as described in porcine skin (Marquet et al., 2014), lung (Maisonasse et al.,  
437 2016) and blood (Auray et al., 2016, Edwards et al., 2017). This phenotype was also  
438 described by Parra-Sanchez et al. (2018) in tonsil. High levels of FLT3 and XCR1 mRNA  
439 expression confirmed the definition of this subset, and homology across species (Reynolds

440 and Haniffa, 2015) (Summerfield et al., 2015). Secretion of IL-12 and a propensity to drive  
441 TH1 responses have also been linked to this population (Jongbloed et al., 2010) and here, high  
442 levels of IL-12 were associated with cDC1s following CPG stimulation, also demonstrated in  
443 cDC1s from porcine lung (Maisonnette et al., 2016). It was interesting that high levels of IL-  
444 12 was also produced by cDC1s in response to Poly:IC despite the low abundance of TLR3.  
445 Furthermore, all tonsillar populations responded to TLR3 agonist with TNF- $\alpha$ . Clearly the  
446 interaction of DCs, with each other (and possibly any remaining lymphoid cells in the  
447 population) is influencing the cytokine secretion profile in addition to TLR expression. The  
448 assessment of sorted cell subsets may have revealed the genuine cytokine expression profile  
449 for each population, although evaluation of a mixed population of cells permits a more  
450 realistic approach for assessing cytokine secretion patterns *in vivo*.

451

452 The phenotype of the cDC2 lineage was confirmed as MHC-II<sup>high</sup>CD172a<sup>high</sup>CD4<sup>-</sup>  
453 CADM1<sup>low</sup>CD14<sup>-</sup>CD163<sup>-</sup> with a moderate ability to take up and process antigen but a  
454 superior capacity to activate allogeneic naïve CD4 T cells. Activation of CD4 T cells,  
455 moderate CADM1 expression and induction of TH2 responses are hallmarks of this cell  
456 population in porcine lung (Maisonnette et al., 2016) and blood (Auray et al., 2016, Edwards  
457 et al., 2017). PCR analysis of this sorted cell subset revealed FLT3 and ZBTB46 expression  
458 and the highest levels of the transcription factor IRF4, necessary for development of cDC2s  
459 from CD11c progenitor cells in lung and spleen in the mouse (Bajana et al., 2016) and for  
460 promoting CD4<sup>+</sup> T cell responses in humans (Vander Lugt et al., 2014). Finally, TLR  
461 expression across these cells was consistent with what has been observed in porcine blood  
462 cDC2s (Auray et al., 2016) suggesting a conserved TLR expression profile in this population  
463 across several tissues.

464

465 The lineage of the fourth, most prominent CD14<sup>+</sup> cell subset identified in the tonsil (MHC-  
466 II<sup>high</sup>CD172a<sup>high</sup>CD4<sup>-</sup>CADM1<sup>low</sup>CD14<sup>+</sup>CD163<sup>-</sup>) was less clear. Expression of FLT3 and  
467 ZBTB46 would classify them as cDCs rather than pDCs, monocytes and M $\phi$ s (Satpathy et  
468 al., 2012) yet the low expression of MAFB (Bakri et al., 2005) and CSF1R (Sasmono et al.,  
469 2003) and variable expression of IL-1 $\beta$  (Beuscher et al., 1990) favours a myelo-monocytic  
470 cell lineage. Notably, a population of CD163<sup>+</sup> DDC in porcine skin which transcriptomically  
471 aligned to moDCs in human and mouse (Marquet et al., 2014) expressed CSF1R, MAFB and  
472 ZBTB46 suggesting this fourth population may also align with this subset. Furthermore,  
473 expression of CD14 (Boltjes and van Wijk, 2014), FLT3 (Menezes et al., 2016), TNF- $\alpha$   
474 secretion (Segura et al., 2013) and a role in pathogen clearance (high uptake of DQ-OVA)  
475 (Serbina et al., 2003) are consistent with an inflammatory dendritic cell lineage generated  
476 from circulating myelo-monocytic cells as shown by others (Lindstedt et al., 2005).  
477 However, we cannot discount the possibility that these cells might also contain cDC2s, given  
478 that different levels of CADM1 were expressed on these cells and that CD14 has also been  
479 associated with human blood cDC2s (Reynolds and Haniffa, 2015). However, CD14 remains  
480 a marker used to indicate a likely monocytic origin (Collin and Bigley, 2018) and is yet to be  
481 demonstrated as a specific marker for cDC2s in pigs (Maisonnette et al., 2016, Summerfield  
482 et al., 2003, Auray et al., 2016, Edwards et al., 2017). It is also plausible that the two levels  
483 of CADM1 represent two populations of moDCs which have yet to be fully delineated and  
484 therefore assumed to be a single DC subset (Chow et al., 2016). Notably, the dominance of  
485 such a cell population in healthy pigs at slaughter seems counter-intuitive, but while these  
486 pigs are clinically healthy, they are not SPF at slaughter age and as such are subject to  
487 challenge by both environmental stimuli and pig specific pathogens (Crossan et al., 2015).

488 Furthermore, the variety of husbandry practises adopted between farms might explain the  
489 variability in frequency of this population between animals.

490

491 Finally, we detected a population of tonsillar cells expressing MHC-II<sup>high</sup>CD172a<sup>high</sup>CD4<sup>-</sup>  
492 CADM1<sup>low</sup>,CD14<sup>-</sup> and CD163<sup>+</sup>, characterised by a high capacity to capture and process  
493 antigen, a low capacity for naïve T cell stimulation and an absence of FLT3 expression  
494 suggesting these cells to be MØs. This is further supported by the high relative abundance of  
495 CSF1R, MAFB, SIRP $\alpha$  and IL-1 $\beta$  transcripts which is consistent with a MØ lineage.  
496 Notably, the highest level of SIRP $\alpha$  (CD172a) transcripts were associated with MØs, which is  
497 in contrast to the flow cytometry data which demonstrated similar levels of SIRP $\alpha$  surface  
498 expression across macrophages, cDC2s and CD14<sup>+</sup> cells. The reason for this inconsistency is  
499 unclear but might relate to the higher detection sensitivity of RT-qPCR, or that surface  
500 expressed SIRP $\alpha$  expression changes in response to various immune mechanisms following  
501 cell activation (Kong et al., 2007). This subset also showed the highest level of expression of  
502 TLR2, TLR4 and TLR6 (Roy et al., 2014), again consistent with a MØ identity. Interestingly  
503 this was the only cell population which appeared to be present in the crypt, the connective  
504 tissue and the epithelium and is therefore likely to play a significant role in the uptake of  
505 antigens and host defence. Notably, all of the myeloid cell populations were observed in the  
506 area beneath the crypt epithelium indicating that all these cells are well positioned to assist in  
507 the uptake of antigens which have translocated the crypt epithelium, for subsequent T  
508 lymphocyte activation. This is consistent with previous reports reviewed in (Horter et al.,  
509 2003).

510

511 Despite the clear alignment of the myeloid populations with their human and mouse  
512 counterparts, differences were observed. For example, pDCs expressed TLR3 which is  
513 otherwise restricted to the cDC1 cell subsets in mice (Segura et al., 2010) and humans  
514 (Jongbloed et al., 2010) although this has also been reported in porcine blood pDCs (Auray et  
515 al., 2016) and might imply a porcine specific pDC response to a wider set of pathogens.  
516 Furthermore, we demonstrated that cDC1 and cDC2 subsets share a similar capacity to  
517 activate allogeneic CD8 T cells, which is consistent with cDC populations in lung  
518 (Maisonasse et al., 2016) while others have shown that in porcine blood (Edwards et al.,  
519 2017) and lymph DCs in sheep (Contreras et al., 2010), cDC1s are superior at activating CD8  
520 T cells. Perhaps in tonsil and lung, being two of the main portals of pathogen entry, a shared  
521 ability between cDCs populations to stimulate CD8 T cells may be advantageous. We also  
522 report that CD14<sup>+</sup> cells were the most frequent population in the tonsil, closely followed by  
523 cDC1s which is in contrast to other tissues, where cDC2s are typically found to be more  
524 widespread than cDC1s (Maisonasse et al., 2016, Ginhoux et al., 2016). A higher frequency  
525 of cDC1 (compared to cDC2) was also reported in porcine lymphoid tissue (Parra-Sanchez et  
526 al., 2018). The reason for this altered balance of DC subsets remains unclear but could  
527 reflect a local presence of DNA-associated pathogen and thus a requirement for TLR9  
528 expression, a receptor which appears to be specific to cDC1s. Alternatively, this disparity  
529 might just reflect inherent differences between different tissues. Our results demonstrate that  
530 cDC1s populations secrete IL-12 as also shown in the porcine lung (Maisonasse et al., 2016)  
531 while others have shown that in the blood, pDCs secrete the highest levels of IL-12 (Auray et  
532 al., 2016) (Edwards et al., 2017). Due to the scarcity and limited survival of pDC cells  
533 outside the tonsil we were unable to include these cells in our analyses, and therefore can  
534 neither refute nor confirm this for porcine tonsil. Finally, the CD14<sup>+</sup> cells population in the  
535 porcine tonsil was found to be CD163<sup>neg/low</sup> with levels of FLT3 mRNA comparable to  
536 cDC2s. This is in contrast to CD163<sup>low</sup> cells (believed to be moDCs in the lung) which were  
537 negative for FLT3 (Maisonasse et al., 2016). CD163<sup>low</sup> cells in skin were also shown to be

538 negative for FLT3 although expression was still 100 times higher than observed in  
539 macrophages (Marquet et al., 2014). The reasons for this difference are currently unclear  
540 and require further investigation.

541

542 This study has demonstrated a distinction and specialisation between myeloid cell  
543 populations as shown previously by others. However, there is also clearly a degree of  
544 plasticity in both cell phenotype and function. For example CADm1 is expressed on cDC2s,  
545 albeit at levels significantly lower, than associated with cDC1s. We also reported co-  
546 expression of TLR2 4 and 6 across CD14<sup>+</sup> cells cDC2s and macrophage populations  
547 indicating that all three cell subsets are able to recognise and respond to similar invading  
548 pathogens. Clearly as this area of work develops and techniques to delineate myeloid cell  
549 populations become more sophisticated, the association between these identified myeloid  
550 cells may become more apparent and additional cell populations may also emerge. It is likely  
551 that both the anatomical and pro-inflammatory environment will add a further layer of  
552 complexity both to the classification of these cells and their ontogeny. How this added  
553 'flexibility' might then influence DC responses to pathogens entering the tonsil remains to be  
554 explained.

555

556 In summary, this study dissected the myeloid cells present in the porcine palatine tonsil and  
557 identified five distinct populations of the myelo-monocytic and DC lineages; two subsets of  
558 conventional DCs (cDC1s and cDC2s), pDCs, as well as a putative moDC population and  
559 macrophages, with clear homology to human subsets. As such the interaction of tonsillar  
560 myeloid cells with viruses such as classical swine fever, which share many characteristics  
561 with human viral haemorrhagic fever (Meurens et al., 2012), might assist in furthering our  
562 understanding of host-pathogen interaction.

563

564

### 565 **Acknowledgments**

566 The work was supported by Project SE0796 and SE2207 from the UK Department for the  
567 Environment, Food and Rural Affairs. The authors gratefully acknowledge Kirsten Morris,  
568 CSIRO Biosecurity Flagship, Australian Animal Health Laboratory, Geelong, Australia for  
569 the kind gift of recombinant porcine IL-3.

570

571

### 572 **Author contributions**

573 FS, BC and LS contributed to the performance of the experiments, FS also contributed to the  
574 design of the experiments, performed the data analysis and preparation of the manuscript. JE  
575 contributed to the design of the experiments, performed the cell sorts and assisted with the  
576 preparation of the manuscript. SG, HC, DW and FSt contributed to the design of the  
577 experiments and preparation of the manuscript. All authors reviewed the manuscript.

578

579

### 580 **Conflict of interest statement**

581 The authors declare no conflict of interest.

582

583

584

585

586

587

588 Table 1 Primers used for qPCR

Target mRNA	Primer sequence	Reference
CSF1R	Fwd: 5'-TGAACGACTCCAACACTACATTGTCA-3' Rev: 5'-TGTAGACGCAGTCGAAGATGCT-3'	(Marquet et al., 2014)
E2.2	Fwd: 5'-CCTTCTCTCTCAGCAGGCAC-3' Rev: 5'-CAGACGACCCTTTGCTCCAT-3'	Designed
IRF7	Fwd: 5'-TGGCAGCACATACTGGTGAG-3' Rev: 5'-AGTGGGCCTGCATATGGAAC-3'	Designed
XCR1	Fwd: 5'-CGATGCCGTCTTCCACAAG-3' Rev: 5'-GGAACCACTGGCGTTCTGA-3'	(Marquet et al., 2014)
IL-1b	Fwd: 5'-AGAGATGAAGTGCTGCACCC-3' Rev: 5'-ACAGACAAAGTCATCATTGCACG-3'	Designed
IRF4	Fwd: 5'-CCGGCCTGTGAAAATGGTTG-3' Rev: 5'-GGACGTGGTCAGCTCTTTCA-3'	Designed
Zbtb46	Fwd: 5'-GCTGGTGCACAGCAAGGA-3' Rev: 5'-GCGGCCGACATGAACAC-3'	(Marquet et al., 2014)
MAFB	Fwd: 5'-TGCGTTCTTTAGACCAATATGTTATGT-3' Rev: 5'-CACCAATAACTCGCCCGCTAT-3'	(Marquet et al., 2014)
FLT3	Fwd: 5'-	(Marquet et al.,

	TG TTCACGCTGAATATAAGAAGGAA-3' Rev: 5'-GGAGCAGGAAGCCTGACTTG-3'	2014)
SIRP $\alpha$	Fwd: 5'-CTGAGACCATCCGAGTTCCG-3' Rev: 5'-CACGCCACCGTGATAAAGA-3'	Designed
$\beta$ -actin	Fwd: 5'-GACTCAGATCATGTTTCGAGACCTT-3' Rev: 5'-CATGACAATGCCAGTGGTGC-3'	Designed
TLR1	Fwd: 5'-AGATTTTCGTGCCACCCTATG-3' Rev: 5'-CCTGGGGGATAAACAATGTG-3'	(Uddin et al., 2013)
TLR2	Fwd: 5'-TGCTATGACGCTTTCGTGTC-3' Rev: 5'-CGATGGAGTCGATGATGTTG-3'	(Uddin et al., 2013)
TLR3	Fwd: 5'-GAGCAGGAGTTTGCCTTGTC-3' Rev: 5'-GGAGGTCATCGGGTATTTGA-3'	(Uddin et al., 2013)
TLR4	Fwd: 5'-TCATCCAGGAAGGTTTCCAC -3' Rev: 5'-TGTCTCCCACTCCAGGTAG-3'	(Uddin et al., 2013)
TLR5	Fwd: 5'-GGTCCCTGCCTCAGTATCAA-3' Rev: 5'-TGTTGAGAAACCAGCTGACG-3'	(Uddin et al., 2013)
TLR6	Fwd: 5'-TCAAGCATTTGGACCTCTCA-3' Rev: 5'-TTCCAAATCCAGAAGGATGC-3'	(Uddin et al., 2013)
TLR7	Fwd: 5'-TCTGCCCTGTGATGTCAGTC -3' Rev: 5'-GCTGGTTTCCATCCAGGTAA-3'	(Uddin et al., 2013)
TLR8	Fwd: 5'-CTGGGATGCTTGGTTCATCT-3' Rev: 5'-CATGAGGTTGTGCGATGATGG-3'	(Uddin et al., 2013)
TLR9	Fwd: 5'-GGCCTTCAGCTTCACCTTGG-3'	(Auray et al., 2016)

	Rev: 5'-GGTCAGCGGCACAACTGAG-3'	
TLR10	Fwd: 5'-GCCCAAGGATAGGCGTAAAT - 3' Rev: 5'-CTCGAGACCCTTCATTCAGC-3'	(Uddin et al., 2013)

589

590 Abbreviations: IL, interleukin, qPCR, quantitative PCR, TLR, toll-like receptor

591

592 **References**

593 AURAY, G., KELLER, I., PYTHON, S., GERBER, M., BRUGGMANN, R., RUGGLI, N. & SUMMERFIELD, A.  
594 2016. Characterization and Transcriptomic Analysis of Porcine Blood Conventional and  
595 Plasmacytoid Dendritic Cells Reveals Striking Species-Specific Differences. *J Immunol*, 197,  
596 4791-4806.

597 BACHEM, A., GUTTLER, S., HARTUNG, E., EBSTEIN, F., SCHAEFER, M., TANNERT, A., SALAMA, A.,  
598 MOVASSAGHI, K., OPITZ, C., MAGES, H. W., HENN, V., KLOETZEL, P. M., GURKA, S. &  
599 KROCZEK, R. A. 2010. Superior antigen cross-presentation and XCR1 expression define  
600 human CD11c+CD141+ cells as homologues of mouse CD8+ dendritic cells. *J Exp Med*, 207,  
601 1273-81.

602 BAJANA, S., TURNER, S., PAUL, J., AINSUA-ENRICH, E. & KOVATS, S. 2016. IRF4 and IRF8 Act in  
603 CD11c+ Cells To Regulate Terminal Differentiation of Lung Tissue Dendritic Cells. *J Immunol*,  
604 196, 1666-77.

605 BAKRI, Y., SARRAZIN, S., MAYER, U. P., TILLMANN, S., NERLOV, C., BONED, A. & SIEWEKE, M. H.  
606 2005. Balance of MafB and PU.1 specifies alternative macrophage or dendritic cell fate.  
607 *Blood*, 105, 2707-16.

608 BANCHEREAU, J. & STEINMAN, R. M. 1998. Dendritic cells and the control of immunity. *Nature*, 392,  
609 245-52.

610 BEUSCHER, H. U., GUNTHER, C. & ROLLINGHOFF, M. 1990. IL-1 beta is secreted by activated murine  
611 macrophages as biologically inactive precursor. *J Immunol*, 144, 2179-83.

612 BOLTJES, A. & VAN WIJK, F. 2014. Human dendritic cell functional specialization in steady-state and  
613 inflammation. *Front Immunol*, 5, 131.

614 CELLA, M., SALIO, M., SAKAKIBARA, Y., LANGEN, H., JULKUNEN, I. & LANZAVECCHIA, A. 1999.  
615 Maturation, activation, and protection of dendritic cells induced by double-stranded RNA. *J*  
616 *Exp Med*, 189, 821-9.

617 CHOW, K. V., LEW, A. M., SUTHERLAND, R. M. & ZHAN, Y. 2016. Monocyte-Derived Dendritic Cells  
618 Promote Th Polarization, whereas Conventional Dendritic Cells Promote Th Proliferation. *J*  
619 *Immunol*, 196, 624-36.

620 CISSE, B., CATON, M. L., LEHNER, M., MAEDA, T., SCHEU, S., LOCKSLEY, R., HOLMBERG, D., ZWEIER,  
621 C., DEN HOLLANDER, N. S., KANT, S. G., HOLTER, W., RAUCH, A., ZHUANG, Y. & REIZIS, B.  
622 2008. Transcription factor E2-2 is an essential and specific regulator of plasmacytoid  
623 dendritic cell development. *Cell*, 135, 37-48.

624 CONTRERAS, V., URIEN, C., GUITON, R., ALEXANDRE, Y., VU MANH, T. P., ANDRIEU, T., CROZAT, K.,  
625 JOUNEAU, L., BERTHO, N., EPARDAUD, M., HOPE, J., SAVINA, A., AMIGORENA, S., BONNEAU,  
626 M., DALOD, M. & SCHWARTZ-CORNIL, I. 2010. Existence of CD8alpha-like dendritic cells with  
627 a conserved functional specialization and a common molecular signature in distant  
628 mammalian species. *J Immunol*, 185, 3313-25.

629 CROSSAN, C., GRIERSON, S., THOMSON, J., WARD, A., NUNEZ-GARCIA, J., BANKS, M. & SCOBIE, L.  
630 2015. Prevalence of hepatitis E virus in slaughter-age pigs in Scotland. *Epidemiol Infect*, 143,  
631 2237-40.

632 CROZAT, K., GUITON, R., CONTRERAS, V., FEUILLET, V., DUTERTRE, C. A., VENTRE, E., VU MANH, T. P.,  
633 BARANEK, T., STORSET, A. K., MARVEL, J., BOUDINOT, P., HOSMALIN, A., SCHWARTZ-CORNIL,  
634 I. & DALOD, M. 2010a. The XC chemokine receptor 1 is a conserved selective marker of  
635 mammalian cells homologous to mouse CD8alpha+ dendritic cells. *J Exp Med*, 207, 1283-92.

636 CROZAT, K., GUITON, R., GUILLIAMS, M., HENRI, S., BARANEK, T., SCHWARTZ-CORNIL, I., MALISSEN,  
637 B. & DALOD, M. 2010b. Comparative genomics as a tool to reveal functional equivalences  
638 between human and mouse dendritic cell subsets. *Immunol Rev*, 234, 177-98.

639 DEN HAAN, J. M., LEHAR, S. M. & BEVAN, M. J. 2000. CD8(+) but not CD8(-) dendritic cells cross-  
640 prime cytotoxic T cells in vivo. *J Exp Med*, 192, 1685-96.

641 EDWARDS, J. C., EVERETT, H. E., PEDRERA, M., MOKHTAR, H., MARCHI, E., SOLDEVILA, F., KAVEH, D.  
642 A., HOGARTH, P. J., JOHNS, H. L., NUNEZ-GARCIA, J., STEINBACH, F., CROOKE, H. R. &  
643 GRAHAM, S. P. 2017. CD1- and CD1+ porcine blood dendritic cells are enriched for the  
644 orthologues of the two major mammalian conventional subsets. *Sci Rep*, 7, 40942.

645 FAIRBAIRN, L., KAPETANOVIC, R., SESTER, D. P. & HUME, D. A. 2011. The mononuclear phagocyte  
646 system of the pig as a model for understanding human innate immunity and disease. *J*  
647 *Leukoc Biol*, 89, 855-71.

648 GINHOUX, F. & GUILLIAMS, M. 2016. Tissue-Resident Macrophage Ontogeny and Homeostasis.  
649 *Immunity*, 44, 439-49.

650 GINHOUX, F., GUILLIAMS, M. & NAIK, S. H. 2016. Editorial: Dendritic Cell and Macrophage  
651 Nomenclature and Classification. *Front Immunol*, 7, 168.

652 HAMMAD, H., PLANTINGA, M., DESWARTE, K., POULIOT, P., WILLART, M. A., KOOL, M., MUSKENS, F.  
653 & LAMBRECHT, B. N. 2010. Inflammatory dendritic cells--not basophils--are necessary and  
654 sufficient for induction of Th2 immunity to inhaled house dust mite allergen. *J Exp Med*, 207,  
655 2097-111.

656 HORTER, D. C., YOON, K. J. & ZIMMERMAN, J. J. 2003. A review of porcine tonsils in immunity and  
657 disease. *Anim Health Res Rev*, 4, 143-55.

658 JAMIN, A., GORIN, S., LE POTIER, M. F. & KUNTZ-SIMON, G. 2006. Characterization of conventional  
659 and plasmacytoid dendritic cells in swine secondary lymphoid organs and blood. *Vet*  
660 *Immunol Immunopathol*, 114, 224-37.

661 JONGBLOED, S. L., KASSIANOS, A. J., MCDONALD, K. J., CLARK, G. J., JU, X., ANGEL, C. E., CHEN, C. J.,  
662 DUNBAR, P. R., WADLEY, R. B., JEET, V., VULINK, A. J., HART, D. N. & RADFORD, K. J. 2010.  
663 Human CD141+ (BDCA-3)+ dendritic cells (DCs) represent a unique myeloid DC subset that  
664 cross-presents necrotic cell antigens. *J Exp Med*, 207, 1247-60.

665 KARSUNKY, H., MERAD, M., COZZIO, A., WEISSMAN, I. L. & MANZ, M. G. 2003. Flt3 ligand regulates  
666 dendritic cell development from Flt3+ lymphoid and myeloid-committed progenitors to Flt3+  
667 dendritic cells in vivo. *J Exp Med*, 198, 305-13.

668 KASTENMULLER, W., KASTENMULLER, K., KURTS, C. & SEDER, R. A. 2014. Dendritic cell-targeted  
669 vaccines--hope or hype? *Nat Rev Immunol*, 14, 705-11.

670 KONG, X. N., YAN, H. X., CHEN, L., DONG, L. W., YANG, W., LIU, Q., YU, L. X., HUANG, D. D., LIU, S. Q.,  
671 LIU, H., WU, M. C. & WANG, H. Y. 2007. LPS-induced down-regulation of signal regulatory  
672 protein {alpha} contributes to innate immune activation in macrophages. *J Exp Med*, 204,  
673 2719-31.

674 LEON, B., LOPEZ-BRAVO, M. & ARDAVIN, C. 2007. Monocyte-derived dendritic cells formed at the  
675 infection site control the induction of protective T helper 1 responses against Leishmania.  
676 *Immunity*, 26, 519-31.

677 LINDSTEDT, M., LUNDBERG, K. & BORREBAECK, C. A. 2005. Gene family clustering identifies  
678 functionally associated subsets of human in vivo blood and tonsillar dendritic cells. *J*  
679 *Immunol*, 175, 4839-46.



680 MAISONNASSE, P., BOUGUYON, E., PITON, G., EZQUERRA, A., URIEN, C., DELOIZY, C., BOURGE, M.,  
681 LEPLAT, J. J., SIMON, G., CHEVALIER, C., VINCENT-NAULLEAU, S., CRISCI, E., MONTOYA, M.,  
682 SCHWARTZ-CORNIL, I. & BERTHO, N. 2016. The respiratory DC/macrophage network at  
683 steady-state and upon influenza infection in the swine biomedical model. *Mucosal Immunol*,  
684 9, 835-49.

685 MANH, T. P., ALEXANDRE, Y., BARANEK, T., CROZAT, K. & DALOD, M. 2013. Plasmacytoid,  
686 conventional, and monocyte-derived dendritic cells undergo a profound and convergent  
687 genetic reprogramming during their maturation. *Eur J Immunol*, 43, 1706-15.

688 MARQUET, F., BONNEAU, M., PASCALE, F., URIEN, C., KANG, C., SCHWARTZ-CORNIL, I. & BERTHO, N.  
689 2011. Characterization of dendritic cells subpopulations in skin and afferent lymph in the  
690 swine model. *PLoS One*, 6, e16320.

691 MARQUET, F., VU MANH, T. P., MAISONNASSE, P., ELHMOUZI-YOUNES, J., URIEN, C., BOUGUYON, E.,  
692 JOUNEAU, L., BOURGE, M., SIMON, G., EZQUERRA, A., LECARDONNEL, J., BONNEAU, M.,  
693 DALOD, M., SCHWARTZ-CORNIL, I. & BERTHO, N. 2014. Pig skin includes dendritic cell  
694 subsets transcriptomically related to human CD1a and CD14 dendritic cells presenting  
695 different migrating behaviors and T cell activation capacities. *J Immunol*, 193, 5883-93.

696 MENEZES, S., MELANDRI, D., ANSELMINI, G., PERCHET, T., LOSCHKO, J., DUBROT, J., PATEL, R.,  
697 GAUTIER, E. L., HUGUES, S., LONGHI, M. P., HENRY, J. Y., QUEZADA, S. A., LAUVAU, G.,  
698 LENNON-DUMENIL, A. M., GUTIERREZ-MARTINEZ, E., BESSIS, A., GOMEZ-PERDIGUERO, E.,  
699 JACOME-GALARZA, C. E., GARNER, H., GEISSMANN, F., GOLUB, R., NUSSENZWEIG, M. C. &  
700 GUERMONPREZ, P. 2016. The Heterogeneity of Ly6C(hi) Monocytes Controls Their  
701 Differentiation into iNOS(+) Macrophages or Monocyte-Derived Dendritic Cells. *Immunity*,  
702 45, 1205-1218.

703 MEURENS, F., SUMMERFIELD, A., NAUWYNCK, H., SAIF, L. & GERDTS, V. 2012. The pig: a model for  
704 human infectious diseases. *Trends Microbiol*, 20, 50-7.

705 NIZZOLI, G., KRIETSCH, J., WEICK, A., STEINFELDER, S., FACCIOTTI, F., GRUARIN, P., BIANCO, A.,  
706 STECKEL, B., MORO, M., CROSTI, M., ROMAGNANI, C., STOLZEL, K., TORRETTA, S.,  
707 PIGNATARO, L., SCHEIBENBOGEN, C., NEDDERMANN, P., DE FRANCESCO, R., ABRIGNANI, S.  
708 & GEGINAT, J. 2013. Human CD1c+ dendritic cells secrete high levels of IL-12 and potently  
709 prime cytotoxic T-cell responses. *Blood*, 122, 932-42.

710 PARRA-SANCHEZ, H., PUEBLA-CLARK, L., RESENDIZ, M., VALENZUELA, O. & HERNANDEZ, J. 2018.  
711 Characterization and expression of DEC205 in the cDC1 and cDC2 subsets of porcine  
712 dendritic cells from spleen, tonsil, and submaxillary and mesenteric lymph nodes. *Mol*  
713 *Immunol*, 96, 1-7.

714 REYNOLDS, G. & HANIFFA, M. 2015. Human and Mouse Mononuclear Phagocyte Networks: A Tale of  
715 Two Species? *Front Immunol*, 6, 330.

716 ROBBINS, S. H., WALZER, T., DEMBELE, D., THIBAUT, C., DEFAYS, A., BESSOU, G., XU, H., VIVIER, E.,  
717 SELLARS, M., PIERRE, P., SHARP, F. R., CHAN, S., KASTNER, P. & DALOD, M. 2008. Novel  
718 insights into the relationships between dendritic cell subsets in human and mouse revealed  
719 by genome-wide expression profiling. *Genome Biol*, 9, R17.

720 ROY, R., SINGH, S. K., DAS, M., TRIPATHI, A. & DWIVEDI, P. D. 2014. Toll-like receptor 6 mediated  
721 inflammatory and functional responses of zinc oxide nanoparticles primed macrophages.  
722 *Immunology*, 142, 453-64.

723 SALIO, M., CELLA, M., SUTER, M. & LANZAVECCHIA, A. 1999. Inhibition of dendritic cell maturation by  
724 herpes simplex virus. *Eur J Immunol*, 29, 3245-53.

725 SASMONO, R. T., OCEANDY, D., POLLARD, J. W., TONG, W., PAVLI, P., WAINWRIGHT, B. J.,  
726 OSTROWSKI, M. C., HIMES, S. R. & HUME, D. A. 2003. A macrophage colony-stimulating  
727 factor receptor-green fluorescent protein transgene is expressed throughout the  
728 mononuclear phagocyte system of the mouse. *Blood*, 101, 1155-63.

729 SATPATHY, A. T., KC, W., ALBRING, J. C., EDELSON, B. T., KRETZER, N. M., BHATTACHARYA, D.,  
730 MURPHY, T. L. & MURPHY, K. M. 2012. Zbtb46 expression distinguishes classical dendritic

731 cells and their committed progenitors from other immune lineages. *J Exp Med*, 209, 1135-  
732 52.

733 SCHLITZER, A. & GINHOUX, F. 2013. DNGR-ing the dendritic cell lineage. *EMBO Rep*, 14, 850-1.

734 SEGURA, E. & AMIGORENA, S. 2013. Identification of human inflammatory dendritic cells.  
735 *Oncoimmunology*, 2, e23851.

736 SEGURA, E., KAPP, E., GUPTA, N., WONG, J., LIM, J., JI, H., HEATH, W. R., SIMPSON, R. &  
737 VILLADANGOS, J. A. 2010. Differential expression of pathogen-recognition molecules  
738 between dendritic cell subsets revealed by plasma membrane proteomic analysis. *Mol*  
739 *Immunol*, 47, 1765-73.

740 SEGURA, E., TOUZOT, M., BOHINEUST, A., CAPPUCCIO, A., CHIOCCHIA, G., HOSMALIN, A., DALOD,  
741 M., SOUMELIS, V. & AMIGORENA, S. 2013. Human inflammatory dendritic cells induce Th17  
742 cell differentiation. *Immunity*, 38, 336-48.

743 SEGURA, E., VALLADEAU-GUILEMOND, J., DONNADIEU, M. H., SASTRE-GARAU, X., SOUMELIS, V. &  
744 AMIGORENA, S. 2012. Characterization of resident and migratory dendritic cells in human  
745 lymph nodes. *J Exp Med*, 209, 653-60.

746 SERBINA, N. V., SALAZAR-MATHER, T. P., BIRON, C. A., KUZIEL, W. A. & PAMER, E. G. 2003. TNF/iNOS-  
747 producing dendritic cells mediate innate immune defense against bacterial infection.  
748 *Immunity*, 19, 59-70.

749 STEINMAN, L., TZEHOVAL, E., COHEN, I. R., SEGAL, S. & GLICKMAN, E. 1978. Sequential interaction of  
750 macrophages, initiator T lymphocytes and recruited T lymphocytes in a cell-mediated  
751 immune response to soluble antigen. *Eur J Immunol*, 8, 29-34.

752 STEINMAN, R. M. & COHN, Z. A. 1973. Identification of a novel cell type in peripheral lymphoid  
753 organs of mice. I. Morphology, quantitation, tissue distribution. *J Exp Med*, 137, 1142-62.

754 SUMMERFIELD, A., AURAY, G. & RICKLIN, M. 2015. Comparative dendritic cell biology of veterinary  
755 mammals. *Annu Rev Anim Biosci*, 3, 533-57.

756 SUMMERFIELD, A., GUZYLACK-PIRIOU, L., SCHAUB, A., CARRASCO, C. P., TACHE, V., CHARLEY, B. &  
757 MCCULLOUGH, K. C. 2003. Porcine peripheral blood dendritic cells and natural interferon-  
758 producing cells. *Immunology*, 110, 440-9.

759 UDDIN, M. J., KAEWMALA, K., TESFAYE, D., THOLEN, E., LOOFT, C., HOELKER, M., SCHELLANDER, K. &  
760 CINAR, M. U. 2013. Expression patterns of porcine Toll-like receptors family set of genes  
761 (TLR1-10) in gut-associated lymphoid tissues alter with age. *Res Vet Sci*, 95, 92-102.

762 VANDER LUGT, B., KHAN, A. A., HACKNEY, J. A., AGRAWAL, S., LESCH, J., ZHOU, M., LEE, W. P., PARK,  
763 S., XU, M., DEVOSS, J., SPOONER, C. J., CHALOUNI, C., DELAMARRE, L., MELLMAN, I. &  
764 SINGH, H. 2014. Transcriptional programming of dendritic cells for enhanced MHC class II  
765 antigen presentation. *Nat Immunol*, 15, 161-7.

766 VAURE, C. & LIU, Y. 2014. A comparative review of toll-like receptor 4 expression and functionality in  
767 different animal species. *Front Immunol*, 5, 316.

768 VU MANH, T. P., BERTHO, N., HOSMALIN, A., SCHWARTZ-CORNIL, I. & DALOD, M. 2015a.  
769 Investigating Evolutionary Conservation of Dendritic Cell Subset Identity and Functions.  
770 *Front Immunol*, 6, 260.

771 VU MANH, T. P., ELHMOUZI-YOUNES, J., URIEN, C., RUSCANU, S., JOUNEAU, L., BOURGE, M.,  
772 MOROLDO, M., FOUCRAS, G., SALMON, H., MARTY, H., QUERE, P., BERTHO, N., BOUDINOT,  
773 P., DALOD, M. & SCHWARTZ-CORNIL, I. 2015b. Defining Mononuclear Phagocyte Subset  
774 Homology Across Several Distant Warm-Blooded Vertebrates Through Comparative  
775 Transcriptomics. *Front Immunol*, 6, 299.

776 ZUCKERMANN, F. A. & HUSMANN, R. J. 1996. Functional and phenotypic analysis of porcine  
777 peripheral blood CD4/CD8 double-positive T cells. *Immunology*, 87, 500-12.

778  
779

780 **Legends to the figures**

781 **Figure 1. Phenotype of porcine tonsillar myeloid cells.** (A) Dissociated tonsillar cells were  
782 depleted of cells expressing specific lineage markers (CD3, CD21, CD8 $\alpha$  and IgM), and the  
783 subsequent enriched myeloid cells were stained with mAbs and examined by flow cytometry.  
784 Illustrative density plots show the gating strategy: I. Large cells, II. Singlets, III. Lineage  
785 negative, IV. MHC class II V. CD172a. Five myeloid cell populations were identified as  
786 shown by the annotated gates, pDC gated as, MHC-II<sup>low</sup> CD172a<sup>low/neg</sup> CD4<sup>+</sup> CADM1<sup>-</sup> CD14<sup>-</sup>  
787 CD163<sup>-</sup>, a cDC1-like population gated as MHC-II<sup>high</sup> CD172a<sup>low/neg</sup> CD4<sup>-</sup> CADM1<sup>high</sup> CD14<sup>-</sup>  
788 CD163<sup>-</sup>, a putative cDC2 gated as MHC-II<sup>hi</sup>, CD172a<sup>hi</sup>, CADM1<sup>low</sup>, a putative inflammatory  
789 CD14<sup>+</sup> DC gated as, CD172a<sup>hi</sup>, CD163<sup>-</sup>, CD14<sup>+</sup> and putative M $\Theta$ s as, CD172a<sup>hi</sup>, MHC II<sup>+</sup>,  
790 CD163<sup>+</sup>. (B) Flow cytometry histograms showing MHC class II, CD172a, CD4, CD14,  
791 CD163, CADM1 and CD152 (CD80/86) expression associated with each of the five defined  
792 myeloid cell populations. The histograms shown are illustrative for a single pig and are  
793 representative of 6 animals. (C) Plot demonstrating the relative proportion of each of the  
794 defined populations within the MHC II positive gate for six different pigs. Error bars and SD  
795 are shown for each individual population.

796

797 **Figure 2. Expression of DC/M $\Theta$ /monocyte related genes by tonsil myeloid cell**  
798 **populations.** The five identified populations were sorted, mRNA extracted and the  
799 expression of several DC/M $\Theta$  associated gene transcripts by the different populations  
800 assessed. mRNA expression levels of E2.2, IRF7, XCR1, IRF4, FLT3, ZBTB46, CSF1R,  
801 MAFB, SIRPa and Il-1b were evaluated by quantitative real-time RT-PCR (qRT-PCR).  
802 Gene expression was normalised to BACT ( $\beta$ -actin) and the relative expression of each gene  
803 was calculated with the  $2^{-\Delta C_t}$  formula using the mean  $C_t$  values from duplicate samples. For  
804 each pig, data is expressed in arbitrary units (AU) obtained by assigning a value of 100 to the  
805 population giving the maximum level of expression and the remaining populations were  
806 compared to it for each gene. Each point on the graph represents the normalised  $2^{-\Delta C_t}$  value  
807 from each cell population from each individual animal. This experiment was performed on a  
808 minimum of 3 animals in more than three independent experiments. Statistical analysis was  
809 performed by a one-way ANOVA and statistical significance is defined by \*\*\*\*p<0.0001,  
810 \*\*\*p<0.001, \*\*p<0.01 and \*p<0.05.

811

812 **Figure 3. Costimulatory molecule expression following 4-hour culture.** The enriched  
813 tonsillar myeloid cells were stained, before and after culture, with the same antibody panel  
814 and gated as described above. Cells were also stained for fusion protein CD152 (CD80/86)  
815 expression to indicate cell maturation. Bar graphs showing the MFI values for CD80/86 and  
816 MHC class II corresponding to each of the defined myeloid populations. Values shown are  
817 from 8 individual pigs and error bars represent 1 SD. Values were compared using a two-way  
818 ANOVA and significance indicated by \*\*\*\*p<0.0001, \*p<0.05.

819

820

821 **Figure 4. Evaluation of Toll-like Receptors (TLRs) expression and cytokine responses to**  
822 **TLR ligands.** The five populations were sorted and the mRNA was extracted to evaluate the  
823 expression of TLRs 1 to 10 by quantitative real-time PCR (qPCR). Each TLR gene  
824 expression level was normalised to  $\beta$ -actin and the relative expression of each gene was  
825 calculated with the  $2^{-\Delta C_t}$  formula using the mean  $C_t$  values from duplicate samples. For each  
826 pig, data is expressed in arbitrary units (AU) obtained by assigning a value of 100 to the  
827 population giving the maximum level of expression and the remaining populations were  
828 compared to it for each gene. Each point on the graph represents the normalised  $2^{-\Delta C_t}$  value  
829 from each individual animal. This experiment was performed on 3 or 4 animals in three  
830 independent experiments. Statistical analysis was performed by a one-way ANOVA and  
831 statistical significance is shown by \*\*\*\* $p < 0.0001$ , \*\*\* $p < 0.001$ , \*\* $p < 0.01$  and \* $p < 0.05$ .

832

833 **Figure 5. Evaluation of antigen processing and T cell stimulatory capacity (A).**  
834 Differential endocytosis between cell populations was evaluated with OVA-DQ-FITC by  
835 culture of lineage depleted myeloid cells for 1.5 hours at 37°C (and 4°C) and APC  
836 fluorescence was assessed by flow cytometry. Histogram shows the mean percentage of cells  
837 taking up DQ from 8 pigs (each tested in triplicate), following subtraction of non-specific  
838 fluorescence (uptake at 4°C) for each cell population from 3 independent experiments. CD4  
839 T cells were also assessed as a negative control. **(B)** Myeloid cells (APC) were sorted and  
840 PBMCs from allogeneic animals were stained with Violet CellTrace and mixed at a APC:T  
841 cell ratio of 1:10 before being culture for 5 days at 37°C. Proliferation of CD3<sup>+</sup>CD4<sup>+</sup> (CD4 T  
842 cells), CD3<sup>+</sup>CD4<sup>-</sup>CD8 $\alpha$ <sup>+</sup> (CD8 T cells) and CD3<sup>+</sup>CD4<sup>+</sup>CD8 $\alpha$ <sup>+</sup> (memory T cells) was  
843 evaluated by flow cytometry. A value of 100 was assigned to the population with the highest  
844 proliferation value and all other populations were compared to this value (and repeated for  
845 each pig). Data is from 3 separate experiments and a minimum of four different animals for  
846 each cell type. A one-way ANOVA was performed and statistical significance is described by  
847 \*\*\*\* $p < 0.0001$ , \*\*\* $p = 0.0002$ , \*\* $p = 0.0016$  and \* $p = 0.0108$ . **(C)** Isolated tonsil cells were  
848 depleted for lineage markers (CD3, CD8 $\alpha$ , CD21 and IgM) and stimulated for 12 hours in the  
849 presence of TLR agonists CpG, Poly I:C or LPS. After incubation, the myeloid populations  
850 were defined using the same antibody panel as described above. IL-12 (top panel) and TNF-  
851  $\alpha$  (bottom panel) secretion was assessed by intracellular staining and flow cytometry. For  
852 each cell population, each point represents a single pig and the horizontal line represents the  
853 mean of at least 7 pigs tested in 3 independent experiments. The mean cytokine secretion of  
854 non-stimulated cells, was subtracted from each of the relevant data points. **(D)**  
855 Representative flow cytometry dot plots, showing IL-12 and TNF $\alpha$  secretion associated with  
856 cDC1 and CD14<sup>+</sup> cells respectively following CpG stimulation.

857 **Figure 6. In situ localisation of the CD14<sup>+</sup> cells and plasmacytoid dendritic cells in**  
858 **porcine palatine tonsil.** CD14<sup>+</sup> cells and pDCs were localised by confocal microscopy  
859 following ethanol fixation of tonsil slices. The areas assessed included the follicle (F), the  
860 interfollicular region (IFA), the crypt (C), and the epithelium (E). The tissue was stained  
861 using panel 1 antibodies; white arrow CD14<sup>+</sup> cells and yellow arrow pDCs Images are  
862 representative of at least two images from each section, from three different pigs. Objective  
863 used: (A) x63 oil immersion. Scale bars as shown.

864 **Figure 7. In situ localisation of conventional dendritic cells and macrophages in porcine**  
865 **palatine tonsil.** Two conventional dendritic cell subsets and macrophages were localised by  
866 confocal microscopy following ethanol fixation of tonsil slices. The areas assessed included

867 the follicle (F), the interfollicular region (IFA), the crypt (C), the connective tissue (CT) and  
868 the epithelium (E). Tissue stained using panel two antibodies; blue arrow cDC1, white arrow  
869 cDC2, yellow arrow macrophages. Images are representative of at least two images from  
870 each section, from three different pigs. Objective used: x40 oil immersion. Scale bars as  
871 shown.

872

In review

Figure 1.TIF

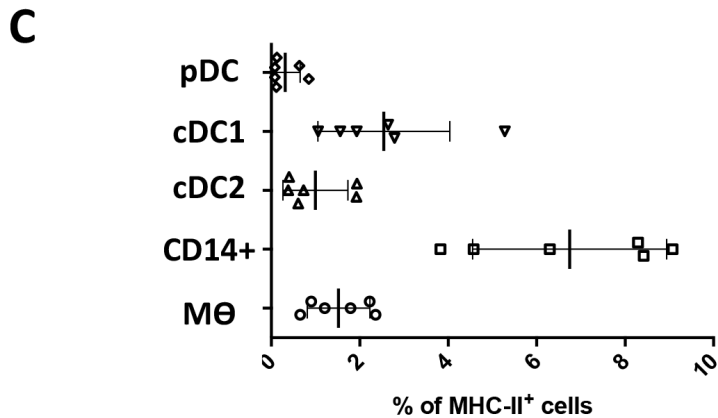
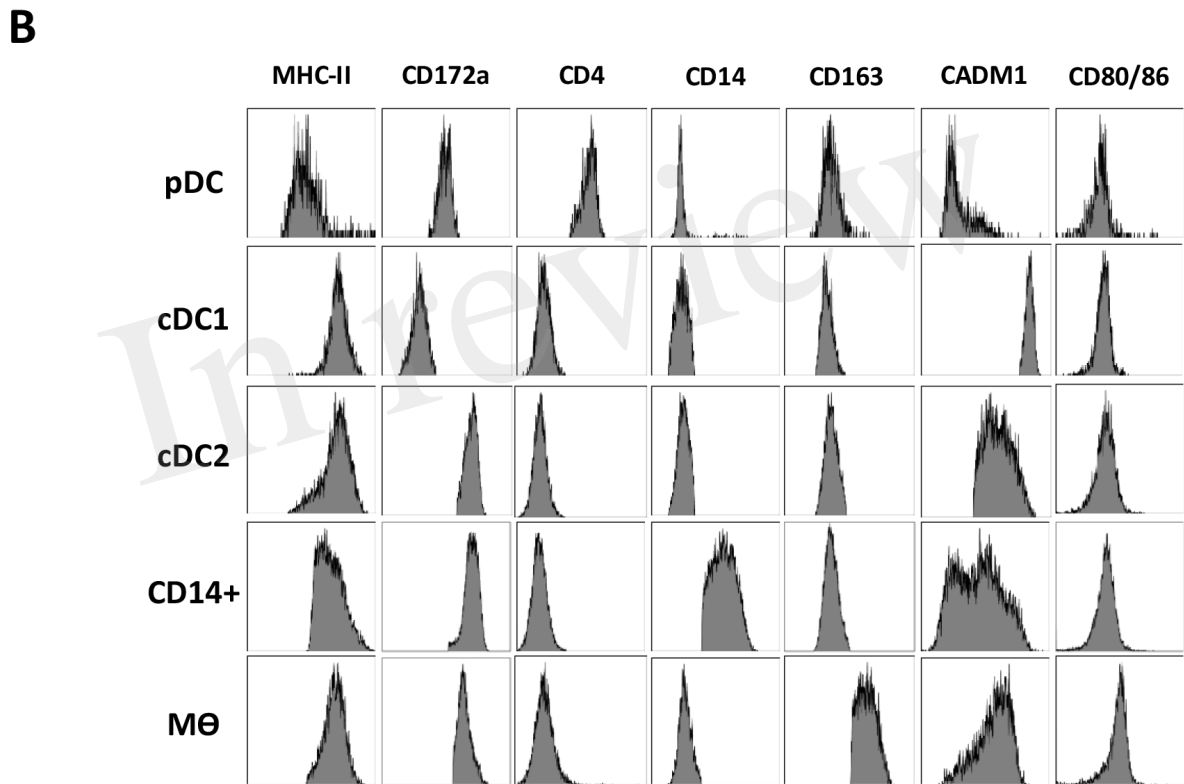
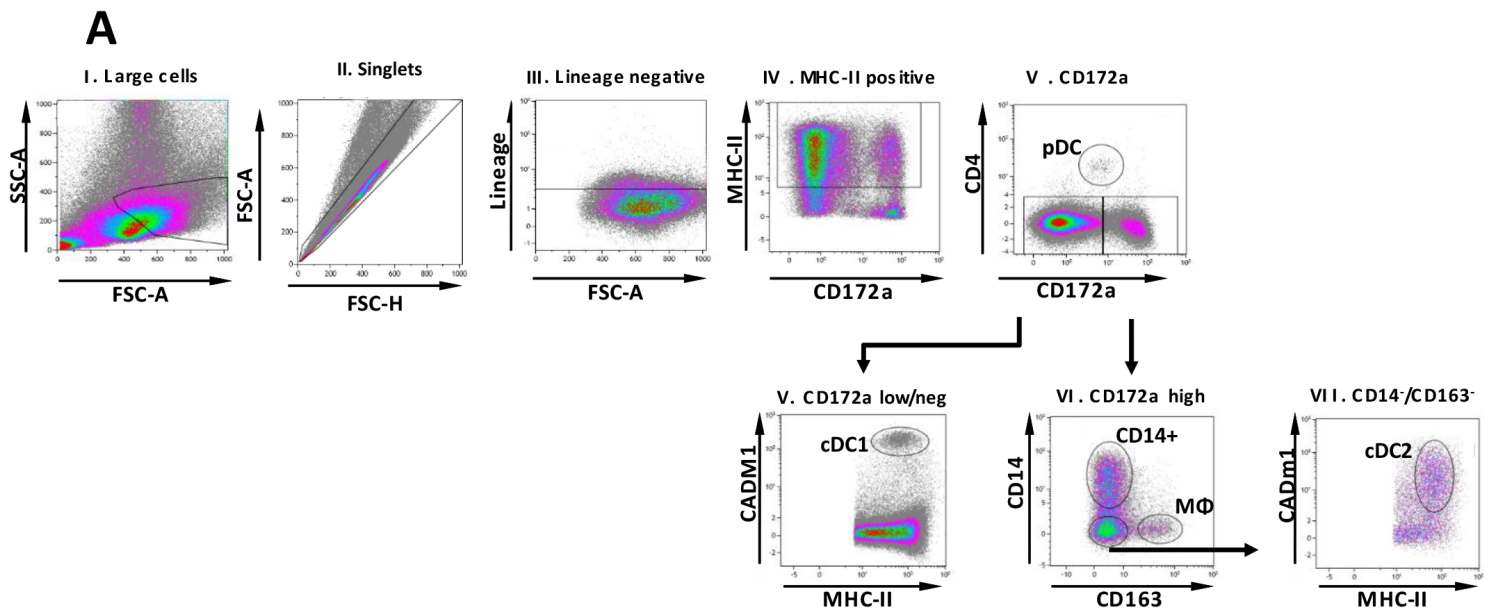


Figure 1.

Figure 2.TIF

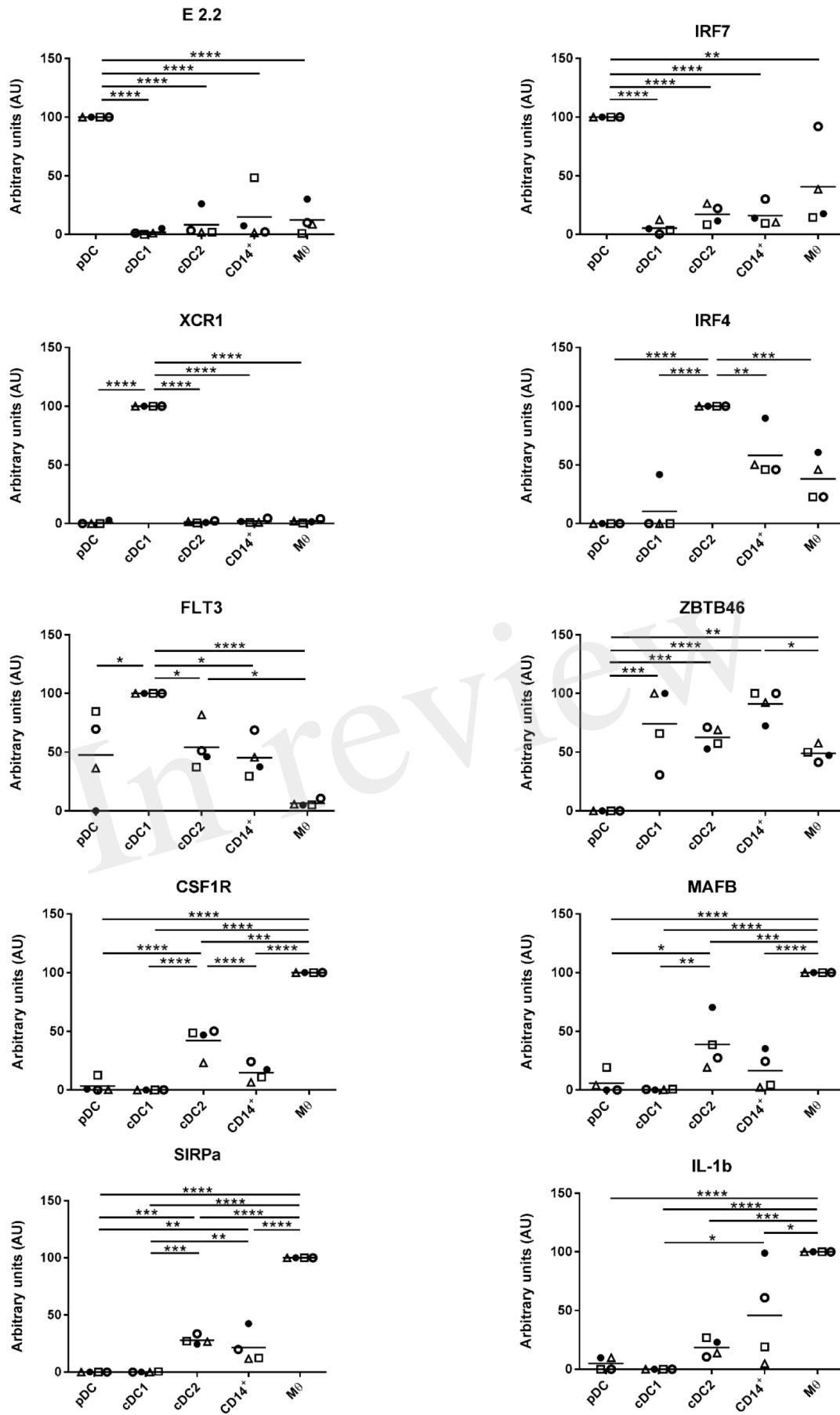


Figure 2

Figure 3.TIF

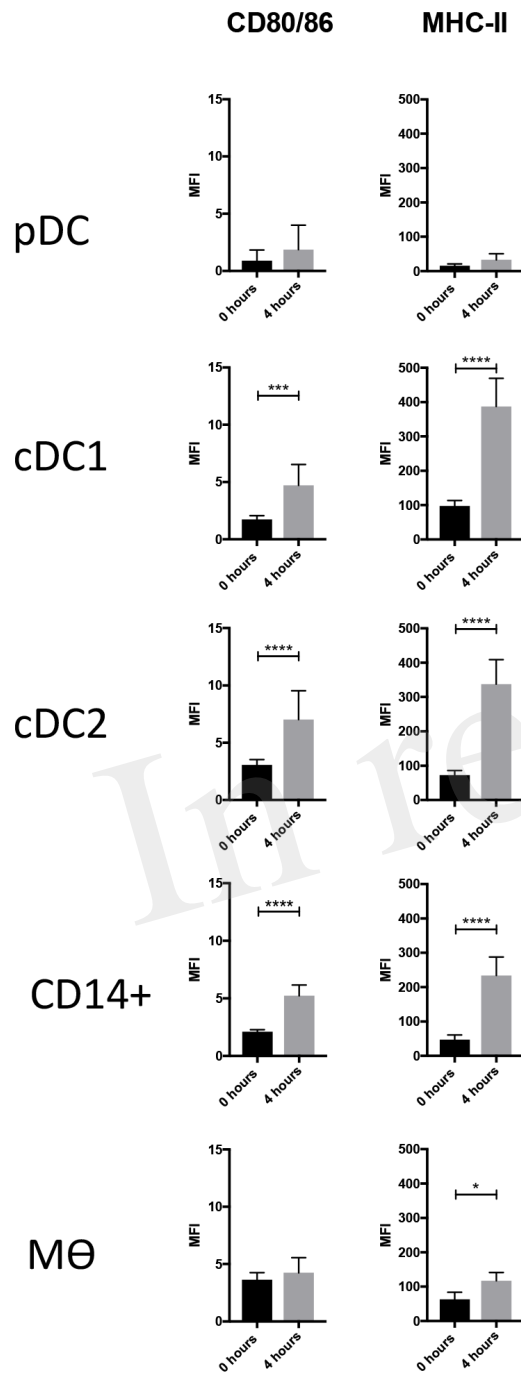


Figure 3.



Figure 4.TIF

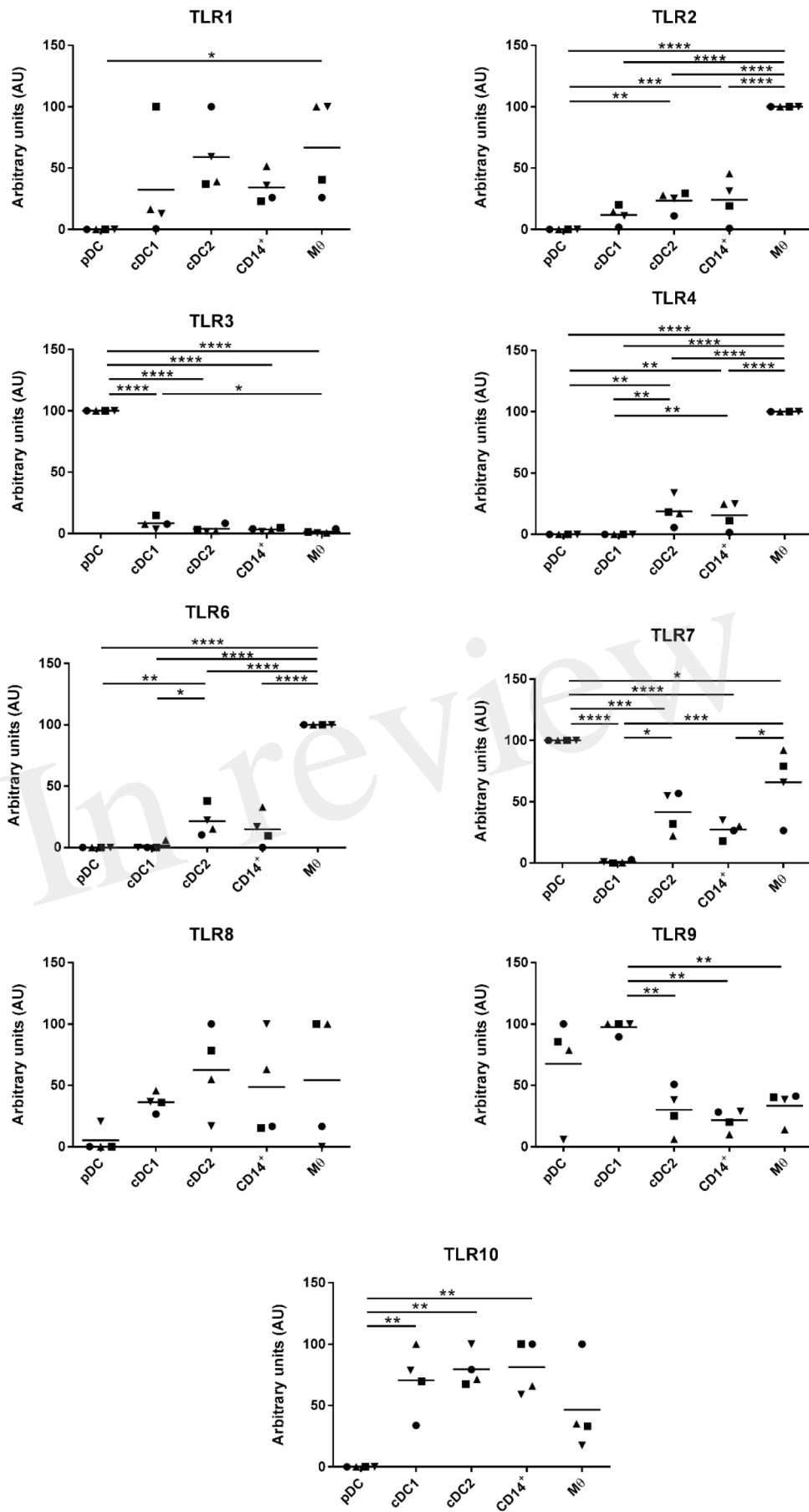


Figure 4.

Figure 5.TIF

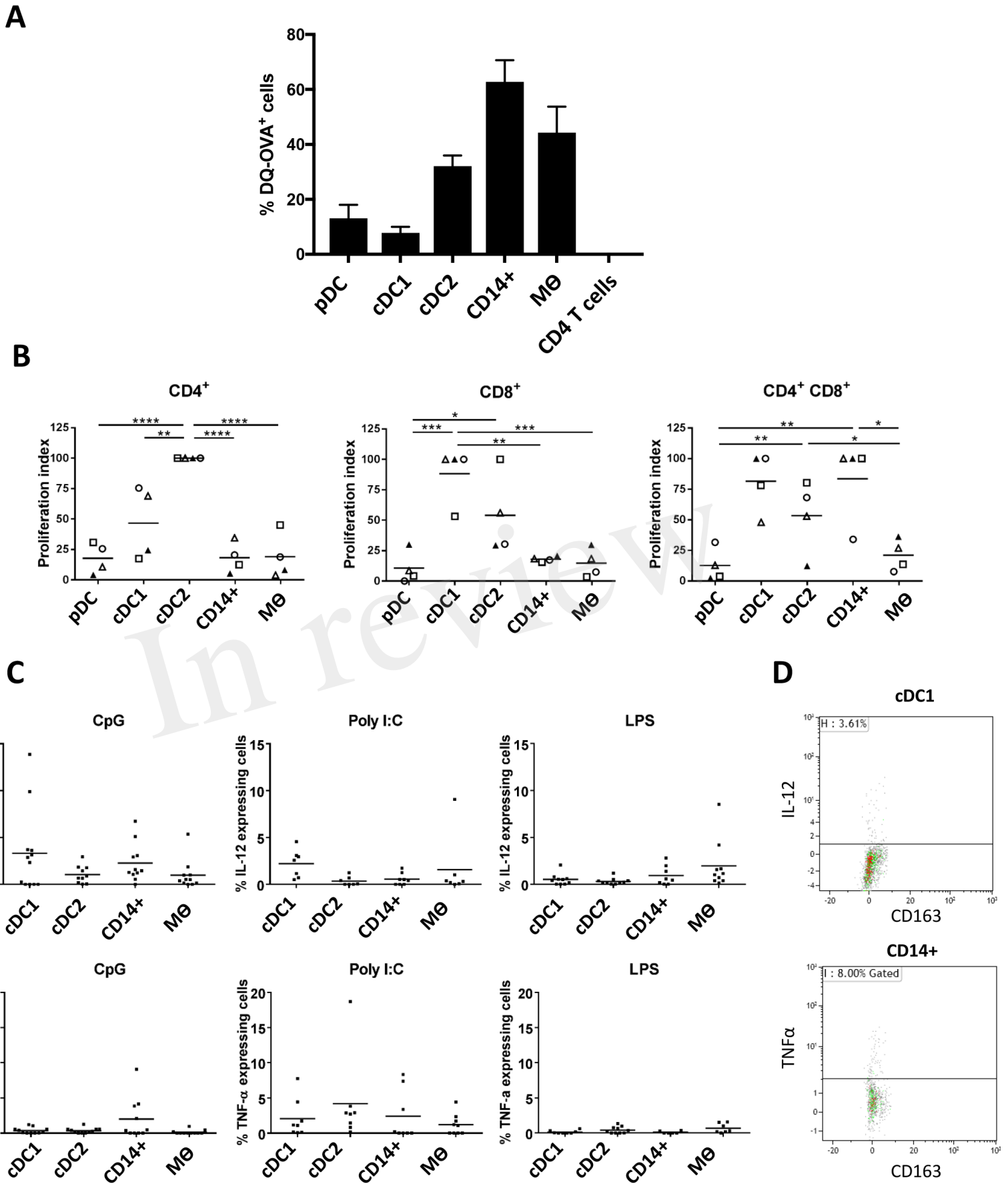


Figure 5.

Figure 6.TIF

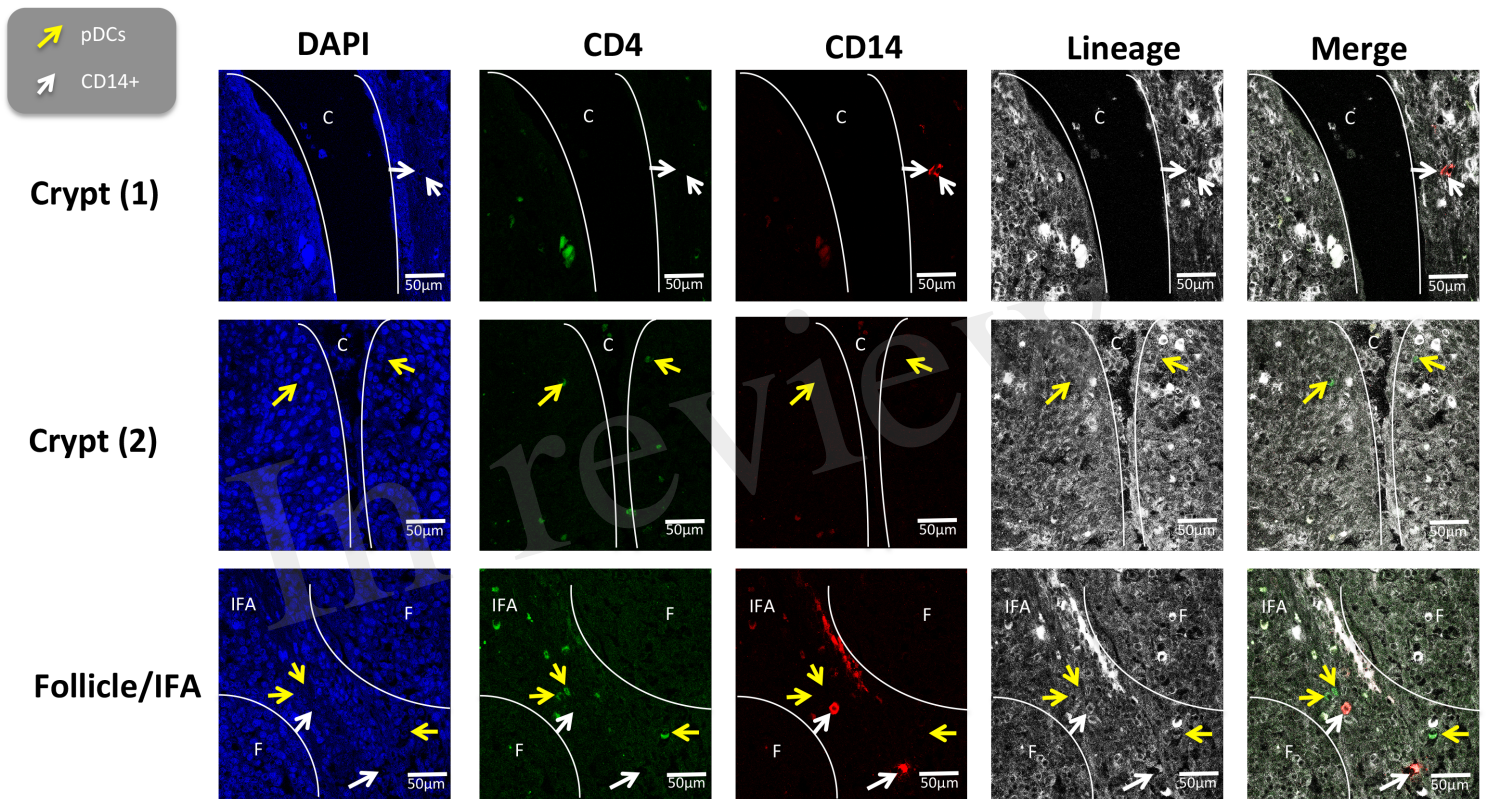


Figure 7.TIF

